

NASA Technical Memorandum 81822

(NASA-TM-81822) THERMAL PERFORMANCE OF A
MECHANICALLY ATTACHED ABLATOR TILE FOR
ON-ORBIT REPAIR OF SHUTTLE TPS (NASA) 51 p
HC A04/MF A01 CSCL 22B

N80-26373

Unclas
GJ/16 23645

THERMAL PERFORMANCE OF A MECHANICALLY ATTACHED
ABLATOR TILE FOR ON-ORBIT REPAIR OF SHUTTLE TPS

STEPHEN S. TOMPKINS, CLAUD M. PITTMAN,
AND ALBERT B. STACEY, JR.

MAY 1980



NASA

National Aeronautics and
Space Administration

Langley Research Center
Hampton, Virginia 23665

THERMAL PERFORMANCE OF A MECHANICALLY ATTACHED ABLATOR TILE FOR
ON-ORBIT REPAIR OF SHUTTLE TPS

BY

STEPHEN S. TOMPKINS

CLAUD M. PITTMAN

ALBERT B. STACEY, JR.

ABSTRACT

The reusable surface insulation (RSI) material used in the primary thermal protection system (TPS) of the space shuttle orbiter is susceptible to damage. If any of the RSI tiles on the orbiter are significantly damaged or lost during ascent, the damaged or lost tiles must be repaired or replaced prior to entry. One approach to replacing a damaged or missing RSI tile is being developed at the NASA-Langley Research Center. This approach consists of mechanically attaching a tile of ablation material in the place of the RSI tile.

The thermal performance of this type of repair tile has been evaluated in a simulated entry heating environment. The test specimen consisted of the ablator repair tile mechanically fastened to the SIP and surrounded by RSI tiles. The evaluation of the thermal performance was based on the temperature response of the fastener, the back-surface temperatures of the specimen, the surface and char integrity of the ablator, and the predicted performance of the repair tile in the flight environment. Based on these results, the following comments can be made.

1. Neither the mechanical fastener nor the fastener tool access hole appeared to significantly affect the thermal performance of the ablator tile.
2. Neither the presence of the fastener tool access hole nor the size of the hole (3/16- and 1/4-inch diameter) appeared to affect

the surface recession or the char integrity, although the temperature of the fastener increased about 7 percent faster with the larger hole compared to the smaller hole.

3. When the ablator tile protruded 1/8-inch above the surrounding RSI tiles, the forward facing steps caused significant inflow of hot gas down the ablator-RSI joints and this inflow caused greatly increased back-surface temperatures.

INTRODUCTION

The reusable surface insulation (RSI) material used in the primary thermal protection system (TPS) of the space shuttle orbiter is extremely susceptible to damage. If any of the RSI tiles on the orbiter are significantly damaged or lost during ascent, the damaged or lost tiles must be repaired or replaced prior to entry. This repair or replacement must be done in-orbit, by an astronaut.

One approach to replacing a damaged or missing RSI tile is being developed at the NASA-Langley Research Center. This approach consists of mechanically attaching a tile of ablation material in the place of the RSI tile. The purpose of this paper is to briefly describe the attachment mechanism and present the results from an experimental and analytical study of the thermal performance of the mechanically attached ablation tile during simulated entry heating.

UNITS

The units for the physical quantities used herein are given in the U.S. Customary Units. Appendix A is included for the purpose of conversion to the International System of Units.

MECHANICAL ATTACHMENT MECHANISM

The strain isolation pad (SIP), required for the current RSI tiles will probably remain on the shuttle orbiter skin if an RSI tile is lost. An ablative heat shield tile can be mechanically attached to the SIP without affecting the aluminum structure or the surrounding RSI tiles.

A mechanical fastener has been developed to attach an ablation material tile quickly and easily to a layer of SIP which is bonded to the aluminum skin of the vehicle. The attachment concept consists of a mechanical fastener in conjunction with a high temperature elastomeric contact adhesive. The contact adhesive was not used in this study because the test specimens needed to be easily removable from the specimen holder. The fastener, shown in figure 1(a), consists of three parts, two rotating and one stationary. The stationary part, shown in the center of the figure, is a flanged sleeve made of aluminum. The upper rotating part, which is 17-4 PH stainless steel, has a flange which shoulders on the aluminum sleeve, external threads on the cylindrical portion, and a small square hole through the

part. The lower rotating part is a 17-4 PH stainless steel internally threaded sleeve with a small square hole in the base and four cloverleaf-like arms. Each arm is sharpened on the end and the outer portion of each arm is bent down. The upper rotating part threads into the lower rotating part.

The manner in which the fastener is used to attach ablator tiles to the SIP is shown in figure 1(b). A small hole is drilled completely through the ablator tile. A larger hole is then drilled in the bottom of the ablator tile to accept the shank of the assembled fastener. This hole is drilled deep enough so that the aluminum flange can be recessed sufficiently to prevent the bent, sharpened ends of the cloverleaf from extending below the ablator. The stationary aluminum part is bonded to the ablator with a suitable adhesive. RTV 560 elastomeric adhesive was used in this study.

The ablator tile is attached to the SIP by placing the tile-fastener assembly on the SIP. An attachment tool, which consists of a handle and a small rod which has been squared for a short distance at the end, is inserted through the small hole in the top of the ablator tile down into the square hole in the upper rotating part. The upper rotating part is unscrewed about one and one-half turns which permits the cloverleaf part to go down against the SIP. The attachment tool is then inserted further until it engages the square hole in the cloverleaf part. A 90 degree turn of the attachment tool makes the cloverleaf prongs

bite into the SIP. The attachment tool is then withdrawn until it engages only the upper part. The upper part is then screwed down, which not only locks the cloverleaf in place. but also pulls the ablator tile down snugly against the SIP.

Tensile tests have shown that each fastener will support a tensile load of more than 50 lbs. When a tensile load is applied, deformation appears to be mostly in the SIP rather than in the fastener.

THERMAL PROTECTION MATERIALS

The Viking ablative heat shield material was selected as the best available ablator for this study. For the on-orbit repair test specimens, the molded version of the Viking material was used. The molded version can be easily cut; therefore, the ablator tile surface can be shaped as needed, to conform to the shuttle outer mold line. This material, fabricated by the Martin Marietta Corp. and designated SLA 561, is an elastomeric material with a density of about 14 lbs/ft³ and consists of a silicone resin, phenolic microspheres, cork, silica fibers and silica microspheres. This material was extensively tested during the Viking Project.

The 9 lb/ft³ RSI material was also used in making the test specimens. This material had the black, reaction-cured glass coating.

TEST SPECIMENS, ENVIRONMENT AND PROCEDURE

The test specimen consisted of a 3-inch square piece of ablation material surrounded by 4 pieces of RSI, 1.2 inches thick, as shown in figure 2. The RSI pieces were bonded to an 0.16 inch thick layer of SIP which was bonded to an 0.125 inch thick canvas/phenolic (Bakelite) carrier panel. The cloverleaf fastener was used to attach the ablator to the SIP. Nine thermocouples (1 to 9) were imbedded in the carrier panel, 10 thermocouples (10 to 19) were bonded on top of the SIP, and one thermocouple (20) was attached to the aluminum flange of the fastener.

Three specimens were tested with the ablator surface flush with the RSI tile surface. One specimen had a 1/4 inch attachment tool hole, one specimen had a 3/16 inch hole, and one specimen had the tool hole plugged with ablator. One specimen was tested with the hole plugged and the ablator sticking up 1/8 inch above the RSI. Each piece of ablator was cut to fit snugly against the RSI tiles. The outward sides of the RSI tiles were coated with adhesives to prevent, as much as possible, flow in through the surface and out the sides of the specimens. The diamond-shaped pattern used with the test specimen simulates the orientation, with respect to the air flow during entry, of the majority of the tiles on the shuttle.

The specimens were mounted on a water-cooled wedge-shaped test fixture, as shown in figure 3. The test fixture was mounted in

the arc-tunnel so that the surface of the test specimen was at a 32 degree angle-of-attack.

The tests were conducted in the supersonic arc-powered tunnel, designated Apparatus B, of the Langley Entry Structures Facility. Apparatus B and the tunnel configuration used for the tests are described in reference 1. The heating rate at the center of the specimen, the total enthalpy and the local pressure at the surface were, respectively, 14 Btu/ft²-s, 1875 Btu/lbm and 0.038 atm. Heating rate and pressure distributions over the 5-inch square test panel are shown in figures 4 and 5, respectively. The heating-rate data were obtained with a square thin-skin calorimeter. Pressure data were obtained with pressure transducers attached to small orifices in a square copper plate. Both the calorimeter and the copper plate were parts of calibration models of the same size and shape as the test models. All tests were conducted in air.

The test procedure for these tests was as follows: the tunnel operating conditions were established and the test environment allowed to stabilize; heating-rate and pressure measurements were made; the model was inserted into the test stream and exposed to the test environment until a temperature of about 760°R was obtained on the fastener flange; the model was then removed from the stream and post-test measurements of heating rate and pressure were made. The measurements showed that the test condition did not change significantly during the tests.

ANALYTICAL METHODS

Two different numerical analyses were used to predict the thermal performance of the ablator tile containing the mechanical attachment device. One was the two-dimensional finite-element thermal analysis, SPAR, described in reference 2 and the other was the one-dimensional finite-difference ablation analysis, CHAP II, described in reference 3. Implicit solution methods were used with both analyses. Thermal properties can be functions of temperature and pressure in both analyses. The ablation analysis, CHAP II, models the complex heat and mass transfer, as well as the thermochemical degradation of the ablator during heating. The SPAR thermal analysis, however, models only the heat transfer. The thermophysical properties used to analyze the ablation material are given in Table I (from refs. 4, 5 and 6). The properties used for the SIP are given in Table II (from ref. 7).

RESULTS AND DISCUSSION

Temperature Responses

Fastener temperature response. - The arc-tunnel tests were terminated when the temperature of the fastener reached about 760 °R. The test times and temperature response of the fastener for each specimen are given in Table III. Note that the test of the

specimen with the ablator protruding was stopped before the fastener reached 760 °R. This test was terminated early because the temperatures at the surface of the SIP in the forward part of the model were extremely high. These high temperatures were a result of hot gas being forced down the ablator/RSI joint by the forward facing step.

The data in Table III show that the larger the fastener tool access hole, the more rapidly the flange reached 760°R. This response was probably caused by inflow of hot gas into the hole and some radiation down the hole. Also, the larger the hole, the lower the maximum temperature and the shorter the time to reach that maximum. This response was simply due to the smaller total heat input to the specimen with the larger holes, and not to any benefit resulting from a larger hole.

Back-surface temperature responses. - Temperatures were measured in the plane between the SIP and the ablator and RSI tiles, as well as in the specimen carrier panel. The temperatures at the end of the heating, the maximum temperatures, and the times of the maximum temperatures for the various locations are shown in figures 6, 7, 8, and 9. (Thermocouple number 20 is on the fastener flange.) In general, at the end of the test, the temperatures between the SIP and TPS tiles were lower for the shorter test times. Except for the specimen with the ablator protruding, none of the temperatures reached 760 R during the heat pulse. The data for the specimen with the

forward facing step (fig. 9b) shows that the locations near the ablator/RSI joint (11, 12, 15, 16, and 18) had very high temperatures. The high temperatures were the result of hot gases deflected by the step down the joint and underneath the TPS tiles.

Except for the protruding-ablator specimen, the temperatures over the carrier panels were fairly uniform at the end of the tests. The inflow of hot gases caused the non-uniform temperatures for the specimen with the step.

Surface Appearance and Char Integrity

Neither the presence of the fastener tool access hole nor the size of the holes tested appeared to significantly affect the surface or char integrity. (See figs. 10, 11 and 12.) The char surface cracked but remained smooth. Very little surface recession occurred. A small amount of char loss was observed in a small area down stream of each hole. The down stream edge of the holes acted as a forward facing step with respect to the local heating. However, the surrounding char was apparently not affected.

After tests of models without the ablator protruding, the surface of the ablator was about 0.05 inch below the RSI tiles and the joints between the ablator and RSI tiles had opened slightly. These dimension changes were probably caused by both ablator char shrinkage during pyrolysis and thermal contraction of the char during cool down.

The thermal performance of the RSI tiles was not adversely affected by the presence of the ablator tile except that ablation products were deposited on the RSI tile surface coating. The chips in the RSI tile seen in figures 10-13 were caused by handling.

The leading edges of the forward facing steps (fig. 13) show significant recession. Molten silica is seen on the leading apex of the ablator tile. Except for the leading edge, the overall surface appearance and char integrity were the same as for the other specimens.

Analytical Results

An attempt was made to predict the thermal response of the SLA 561 ablator tile containing the mechanical fastener device in an arc-tunnel test and for the shuttle design entry trajectory 14414.1C. The purpose of the prediction was to estimate the effects of the fastener on the thermal response of the tile.

Arc-tunnel test.- The one-dimensional CHAP II ablation analysis was used to predict the ground test results since it models the complex ablation processes, even though the heat and mass transfer were multidimensional during the test.

The specimen was analyzed as a one-dimensional block consisting of the SLA 561 ablator, RTV bond line, a layer of 0.16 SIP, RTV bond line and the carrier panel. The heating conditions at the center of the specimen were used in the analysis. Be-

cause the fastener was not included in the analysis, the calculated temperatures were compared to the temperatures measured at locations 1, 14 and 17 (fig. 6) and not to the temperatures at location 20.

The comparison between the measured and calculated temperatures are given in Table IV. The agreement at the end of heating (494 sec.) at locations 14 and 17 (between the SIP and ablator tile) was good. The calculated temperature was only 8 degrees lower than the average temperature at the two locations. This good agreement indicates that the thermal perturbation caused by the fastener is very localized and that the material properties and ablation model used for the SLA 561 are satisfactory.

At 494 seconds, the agreement at thermocouple no. 1 in the carrier panel was only fair because, although the temperature difference is only 8 degrees, the total temperature rise at this location was much smaller. Discrepancies between calculated and measured temperatures at deep locations and long times were primarily caused by difficulties in specifying an accurate back surface boundary condition for a carrier panel adjacent to, but not touching, a water-cooled test fixture.

Predicted flight performance. - The thermal response of the tile with fastener for the design trajectory was calculated with both the CHAP II and SPAR analyses. Only orbiter body point 1030 was considered. The heating rate, enthalpy, pressure, and shear at this point are shown in figure 14.

A schematic of the model used in the SPAR analysis is shown in figure 15. The parts of the fastener were lumped together and treated as a heat sink. Because of the symmetry of the tile, the analysis was restricted to a wedge-shaped slice, with the apex at the center of the fastener.

Since the SPAR analysis does not model the internal mass transfer and thermochemical decomposition, the ablator was modeled as an insulator. This approach has been used successfully for ablators when the surface recession is small or negligible. In this approach, material properties change from those of the uncharred material to those of the charred material at the pyrolysis temperature. The layer of material that has exceeded the pyrolysis temperature retains the properties of the char for all times thereafter.

A comparison of the internal temperature distribution predicted by the ablation analysis and the conduction analysis (along the tile edge, three inches from the fastener) is shown in figure 16. The agreement is satisfactory. The higher temperatures predicted by the conduction analysis were at least partly due to the relatively large element sizes used in the SPAR analysis for these studies. Since these were preliminary calculations, no smaller elements were used.

Two-dimensional temperature distributions predicted by SPAR at three times in the design trajectory are shown in figure 17. At 600 seconds, when peak heating occurred (fig. 17a), the tempera-

ture of the fastener had not changed from the initial value and the depth-wise temperature gradient was uniform throughout the tile. At 1600 seconds, when the end of heating occurred (fig. 17b), the fastener had a definite affect on the local temperatures. The fastener, acting as a heat sink, lowered the temperatures as much as 46 °R below the corresponding temperature at the edge of the tile. The depth-wise temperature gradient near the fastener was also affected. At 4000 seconds, figure 17c, the temperatures near the fastener were still lower than at the tile edge. The calculations showed that the temperatures at the back surface were still rising at 4000 seconds but that the rate of temperature rise was small. Based on these calculations, the fastener does not appear to jeopardizethe thermal performance of the ablator tile. The effects of the non-uniform depth-wise temperature gradient on the thermal stresses in the ablator are not known and should be investigated.

CONCLUDING REMARKS

The thermal performance of a mechanically attached ablator repair tile for the space shuttle orbiter has been evaluated in a simulated entry heating environment. The test specimen consisted of the ablator repair tile mechanically fastened to the SIP and surrounded by RSI tiles. The evaluation of the thermal performance was based on the temperature response of the fastener, the back-surface temperatures of the specimen, the surface and char

integrity of the ablator, and the predicted performance of the repair tile in the flight environment. Based on these results, the following conclusions can be drawn.

1. Neither the mechanical fastener nor the fastener tool access hole appeared to significantly affect the thermal performance of the ablator tile.
2. Neither the presence of the hole nor the size of hole (3/16- and 1/4-inch diameter) appeared to affect the surface recession or the char integrity, although the temperature of the fastener increased about 7 percent faster with the larger hole compared to the smaller hole.
3. When the ablator tile protruded 1/8-inch above the surrounding RSI tiles, the forward facing steps caused significant inflow of hot gas down the ablator-RSI joints and this inflow caused greatly increased back-surface temperatures.

REFERENCES

1. Brown, Ronald D.; and Jakubowski, Antoni K.: Heat-Transfer and Pressure Distributions for Laminar Separated Flows Downstream of Rearward-Facing Steps With and Without Mass Suction. NASA TN D-7430, 1974.
2. Marlowe, M. B., Moore, R. A., and Whetstone, W. D.: SPAR Thermal Analysis Processes Reference Manual, System Level 16, NASA CR 159162, October 1979.

3. Swann, R. T.; Pittman, C. M.; and Smith, J.C.: One-Dimensional Numerical Analysis of the Transient Response of Thermal Protection Systems. NASA TN D-2976, 1965.
4. Anon.: Ablation Material Property Data Book Viking '75 Project. Martin Marietta Co. Rpt TN 3770161, 1972.
5. Anon.: Phase II Ablation Performance Test Report. Martin Marietta Co. Rpt TN 3770110, 1971.
6. Moyer, C. B.; Green, K. A.; and Wool, M. R.: Demonstration of the Range Over Which the Langley Research Center Digital Computer Charring Ablation Program (CHAP) Can Be Used With Confidence. NASA CR-111834, Dec. 1970.
7. Anon.: Materials Properties Manual Vol. 3. Thermal Protection System Materials Data. Prepared by Materials and Processes Group Shuttle Engineering Rockwell International Shuttle Orbiter Division Space Systems Group, May 1979.

APPENDIX A

CONVERSION OF U. S. CUSTOMARY UNITS TO SI UNITS

PHYSICAL QUANTITY	U.S. CUSTOMARY UNITS	CONVERSION FACTOR (*)	SI UNITS (**)
Density	lbm/ft ³	16.018463	kg/m ³
Enthalpy	Btu/lbm	2.32 x 10 ³	J/kg
Heating Rate	Btu/ft ² -s	1.134893x10 ⁴	W/m ²
Pressure	lbf/ft ²	47.88	N/m ²
Specific Heat	Btu/lbm-°R	4.18 x 10 ³	J/kg-K
Temperature	°R	1.8	K
Thermal Conductivity	Btu/ft-s-°R	6.24x10 ³	W/m-k
Thickness	in.	2.54 x 10 ⁻²	m

* Multiply value given in U.S. Customary Units by Conversion factor to obtain equivalent value in SI unit

** Prefixes to indicate multiples of units are as follows:

Prefix	Multiple
centi (c)	10 ⁻²
kilo (k)	10 ³
mega (m)	10 ⁶

TABLE I - THERMOPHYSICAL PROPERTIES FOR SLA 561
VIRGIN MATERIAL

Density (Ref. 4). . . 14.5 lbm/ft³

Thermal Conductivity (ref. 4), Btu/ft-s-°R

<u>Temperature, °R</u>	<u>10⁻⁹ atm</u>	<u>1.3 x 10⁻³ atm</u>	<u>1 atm.</u>
510	6.0 x 10 ⁻⁶	7.1 x 10 ⁻⁶	8.5 x 10 ⁻⁶
560	6.1 x 10 ⁻⁶	7.2 x 10 ⁻⁶	9.0 x 10 ⁻⁶
610	6.1 x 10 ⁻⁶	7.4 x 10 ⁻⁶	9.6 x 10 ⁻⁶
660	6.2 x 10 ⁻⁶	7.5 x 10 ⁻⁶	10.1 x 10 ⁻⁶
710	6.2 x 10 ⁻⁶	7.6 x 10 ⁻⁶	10.6 x 10 ⁻⁶
760	6.2 x 10 ⁻⁶	7.8 x 10 ⁻⁶	11.2 x 10 ⁻⁶
810	6.3 x 10 ⁻⁶	7.9 x 10 ⁻⁶	11.8 x 10 ⁻⁶
860	6.3 x 10 ⁻⁶	8.1 x 10 ⁻⁶	12.3 x 10 ⁻⁶

Specific Heat (ref. 4), Btu/lbm-°R

<u>Temperature, °R</u>	<u>Specific Heat</u>
310	0.211
410	0.250
510	0.275
610	0.289
710	0.299
810	0.301

Pyrolysis Kinetics (ref. 4)

$$m_p = A \exp(-B/T) \text{ where } A = 3510 \text{ lbm/ft}^2\text{-s and } B = 18095 \text{ °R}$$

$$m_p = \text{pyrolysis rate, lbm/ft}^2\text{-s}$$

$$T = \text{temperature, °R}$$

TABLE I (Continued)

PYROLYSIS GASES

Heat of Pyrolysis. 0
 Specific Heat, Btu/lbm-°R. . . . 0.6

CHARRED MATERIAL

Density (ref. 4) 7.98 lbm/ft³
 Emissivity (ref. 4) 0.9
 Thermal Conductivity (ref. 5), Btu/ft-s-°R

<u>Temperature, °R</u>	<u>Thermal Conductivity</u>
400	1.5 x 10 ⁻⁵
1600	1.51 x 10 ⁻⁵
1800	1.64 x 10 ⁻⁵
2000	1.82 x 10 ⁻⁵
2200	2.06 x 10 ⁻⁵
2400	2.40 x 10 ⁻⁵
2600	2.76 x 10 ⁻⁵
2800	3.16 x 10 ⁻⁵
3000	3.60 x 10 ⁻⁵
3200	4.10 x 10 ⁻⁵
3400	4.70 x 10 ⁻⁵
3600	5.41 x 10 ⁻⁵

Table I - (Concluded)

<u>Specific Heat (ref. 4)</u> <u>Temperature, °R</u>	<u>Btu/lbm-°R</u> <u>Specific Heat</u>
600	0.195
800	0.231
1000	0.268
1200	0.297
1400	0.320
1600	0.343
1800	0.363
2000	0.383
2200	0.400
2400	0.413

Oxidation Kinetics (ref. 6)

Order of oxidation1
 Activation temperature76500 °R
 Reaction rate constant 10^{10} lbm/ft²-s-atm

TABLE II - THERMOPHYSICAL PROPERTIES FOR 0.160 SIP
(REF. 7)

Density 9 lbm/ft³

Thermal Conductivity, Btu/ft-s-°R

<u>Temperature, °R</u>	<u>Thermal Conductivity (0.04 atm)</u>
310	3.94 x 10 ⁻⁶
560	6.25 x 10 ⁻⁶
710	7.87 x 10 ⁻⁶
860	9.49 x 10 ⁻⁶
1060	13.2 x 10 ⁻⁶

Specific Heat, Btu/lbm-°R

<u>Temperature, °R</u>	<u>Specific Heat</u>
520	0.23
560	0.26
660	0.34
760	0.45
860	0.57

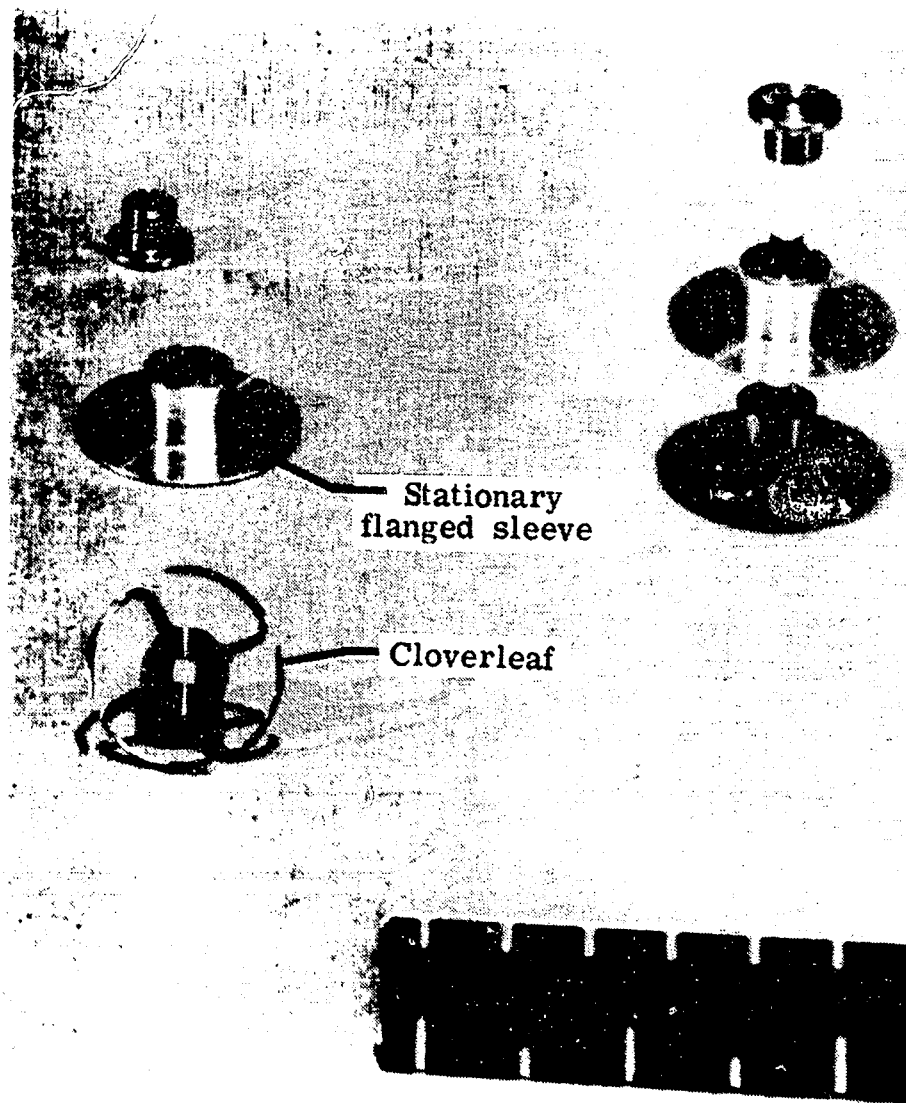
TABLE III - FASTENER TEST TEMPERATURES IN DIFFERENT SPECIMENS
(THERMOCOUPLE NO. 20)

SPECIMEN CHARACTERISTIC	END OF EXPOSURE		MAXIMUM TEMPERATURE	
	TIME, S	TEMPERATURE, °R	TIME, S	TEMPERATURE, °R
3/16" Hole Plugged	494	755	800	837
3/16" Hole Open	450	767	710	821
1/4" Hole Open	420	764	670	811
3/16" Hole Plugged and Ablator Pro- truding 1/8 inch	500 ^a	695	940	845

^a Test stopped due to high temperature at front of specimen at thermocouple no. 11, between the SIP and RSI tile

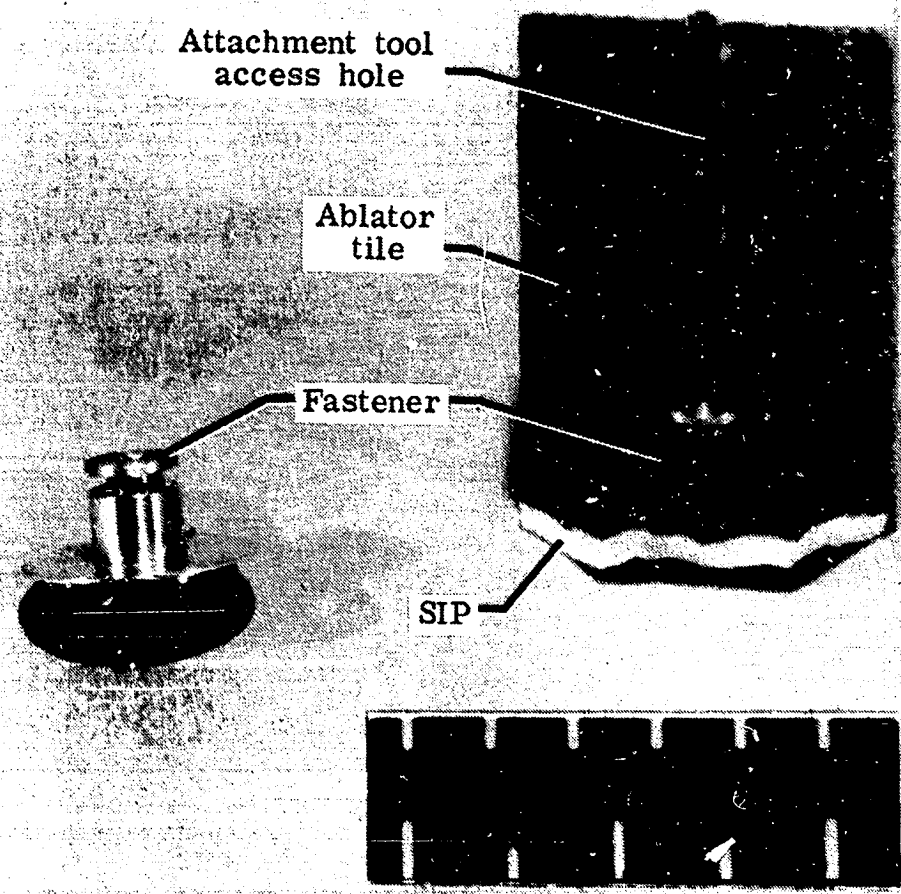
TABLE IV. - COMPARISON OF MEASURED AND CALCULATED TEMPERATURES FOR ARC-TUNNEL TEST (INITIAL TEMPERATURE -- 540 °R)

TIME, s	TEMPERATURES, °R		
	MEASURED		CALCULATED
	NO. 14	NO. 17	
494	568	600	576 658 658
900	---	698	
940	678	---	
494 1010	NO. 1		544 595
	552 641		



(a) Exploded view of mechanical fastener.
Figure 1 - Mechanical attachment mechanism.

ORIGINAL PAGE
OF POOR QUALITY



(b) Mechanical fastener bonded in ablation material.

Figure 1 - Concluded.

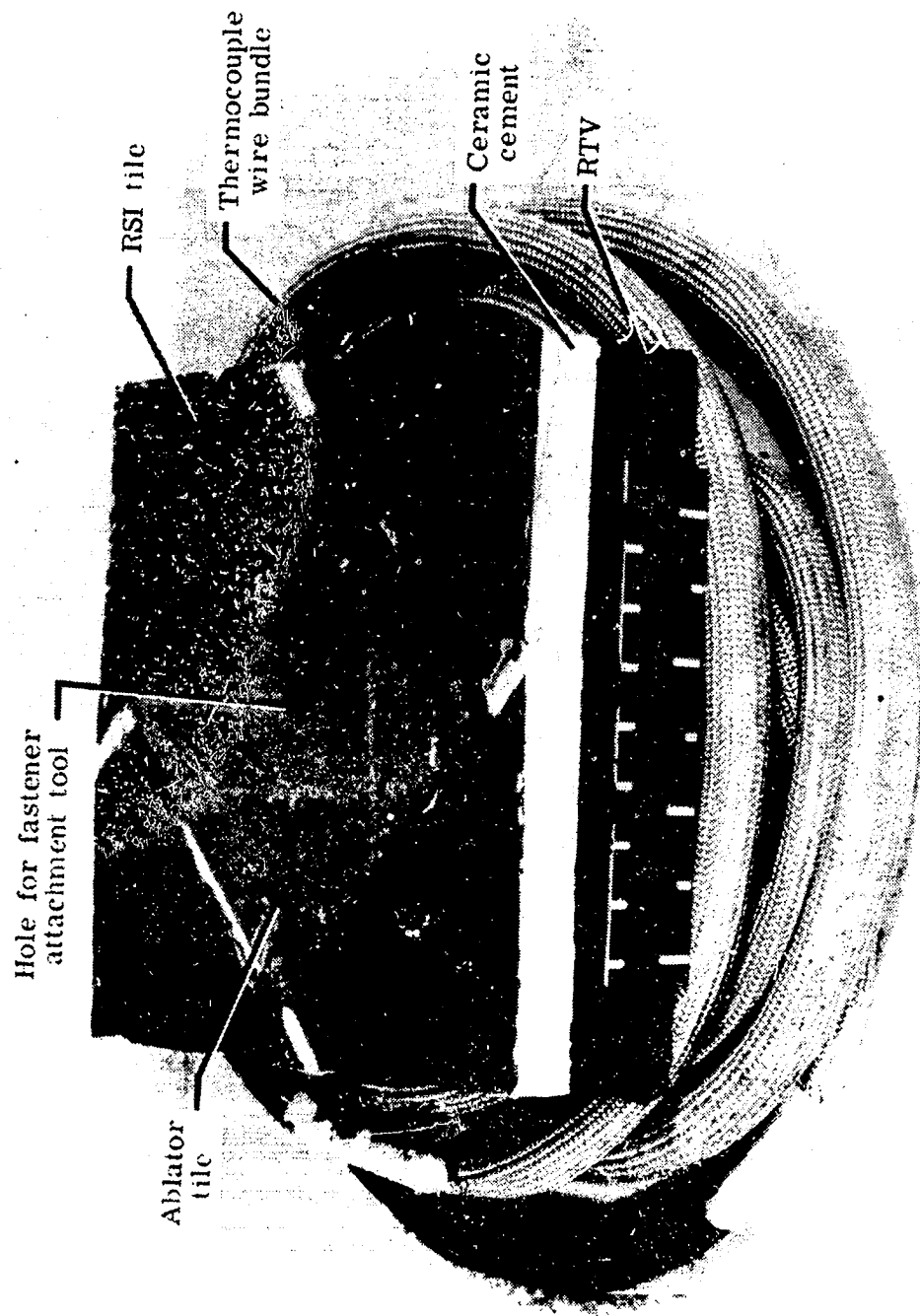


Figure 2 - Test specimen configuration.

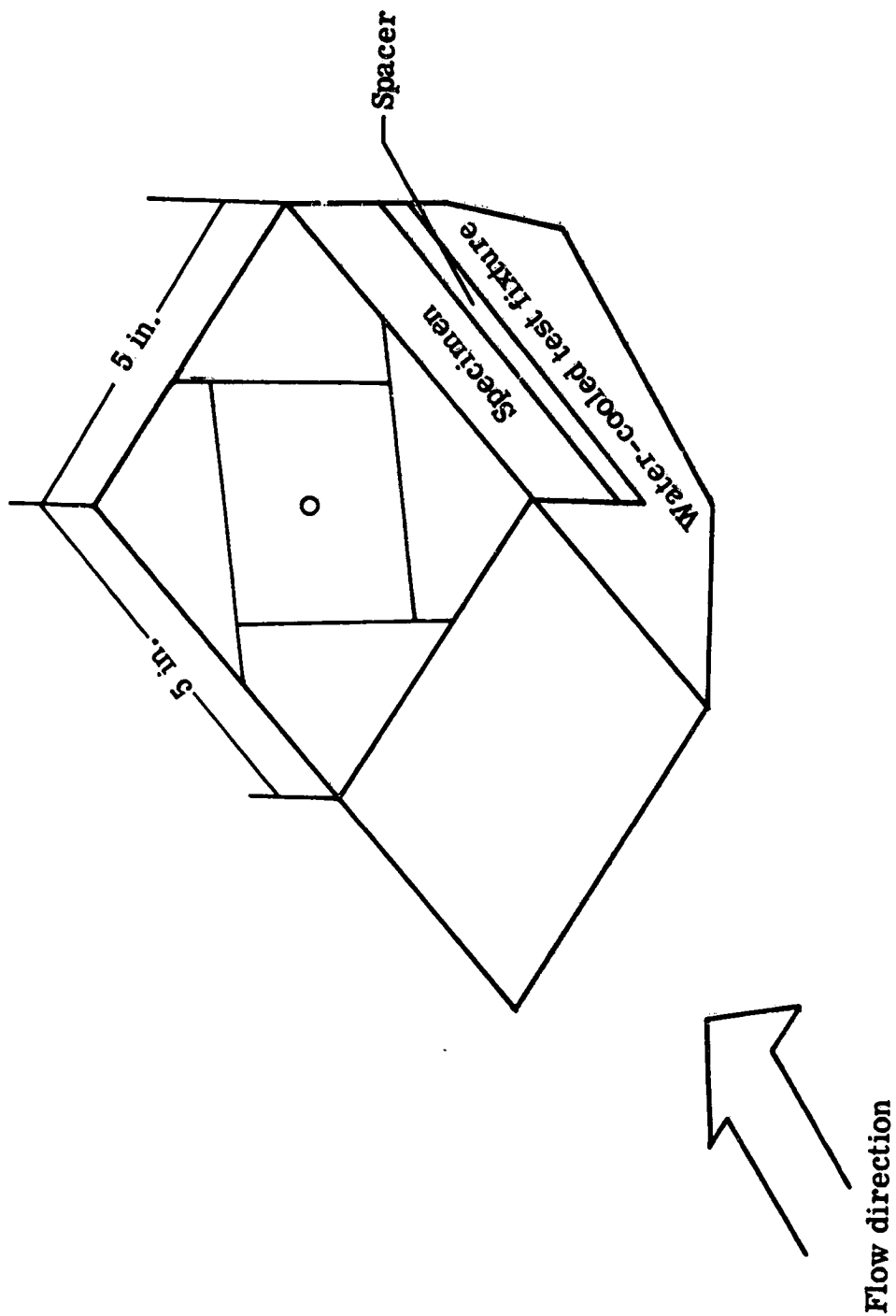


Figure 3.- Specimen mounted on test fixture.

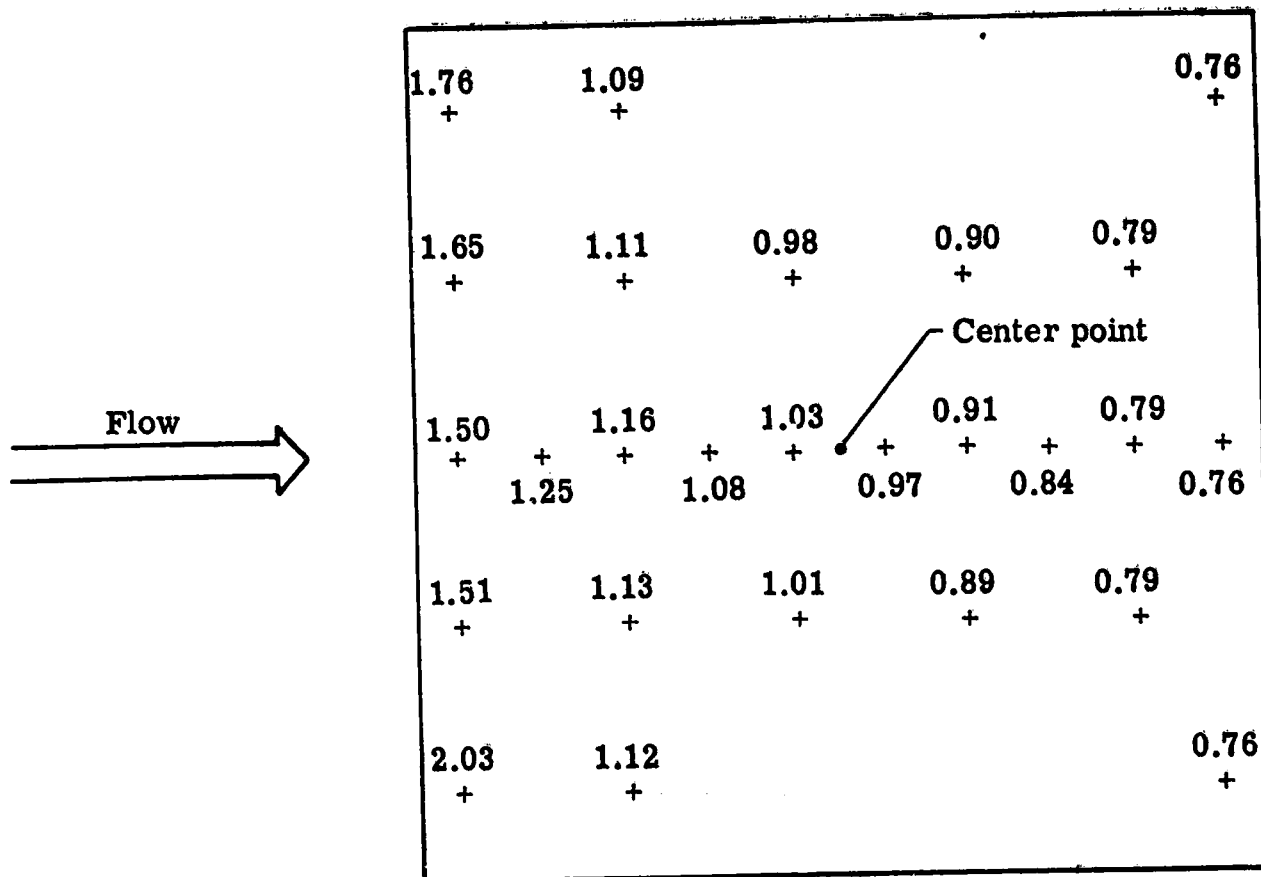


Figure 4.- Typical heating rate distribution normalized to center point.

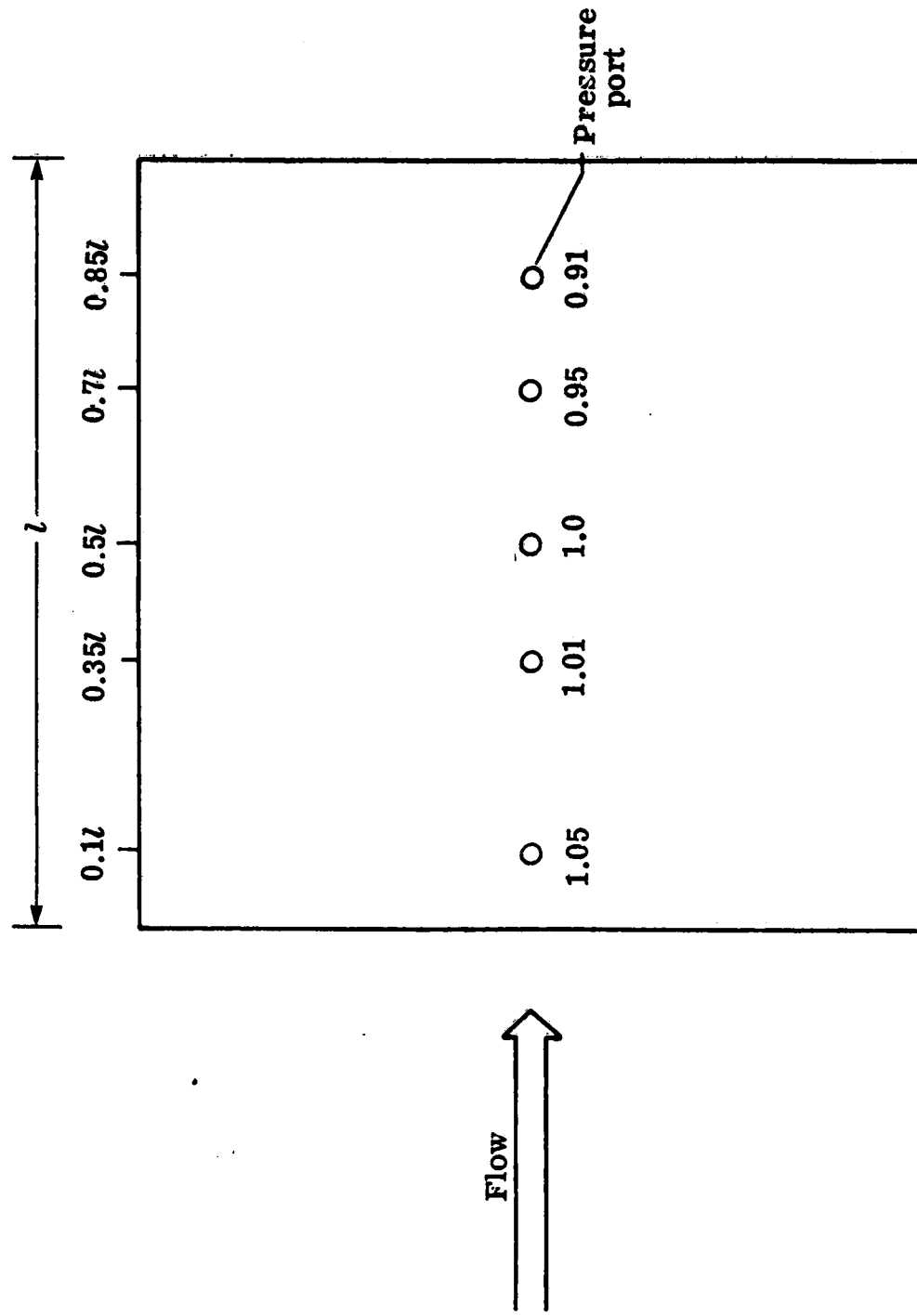
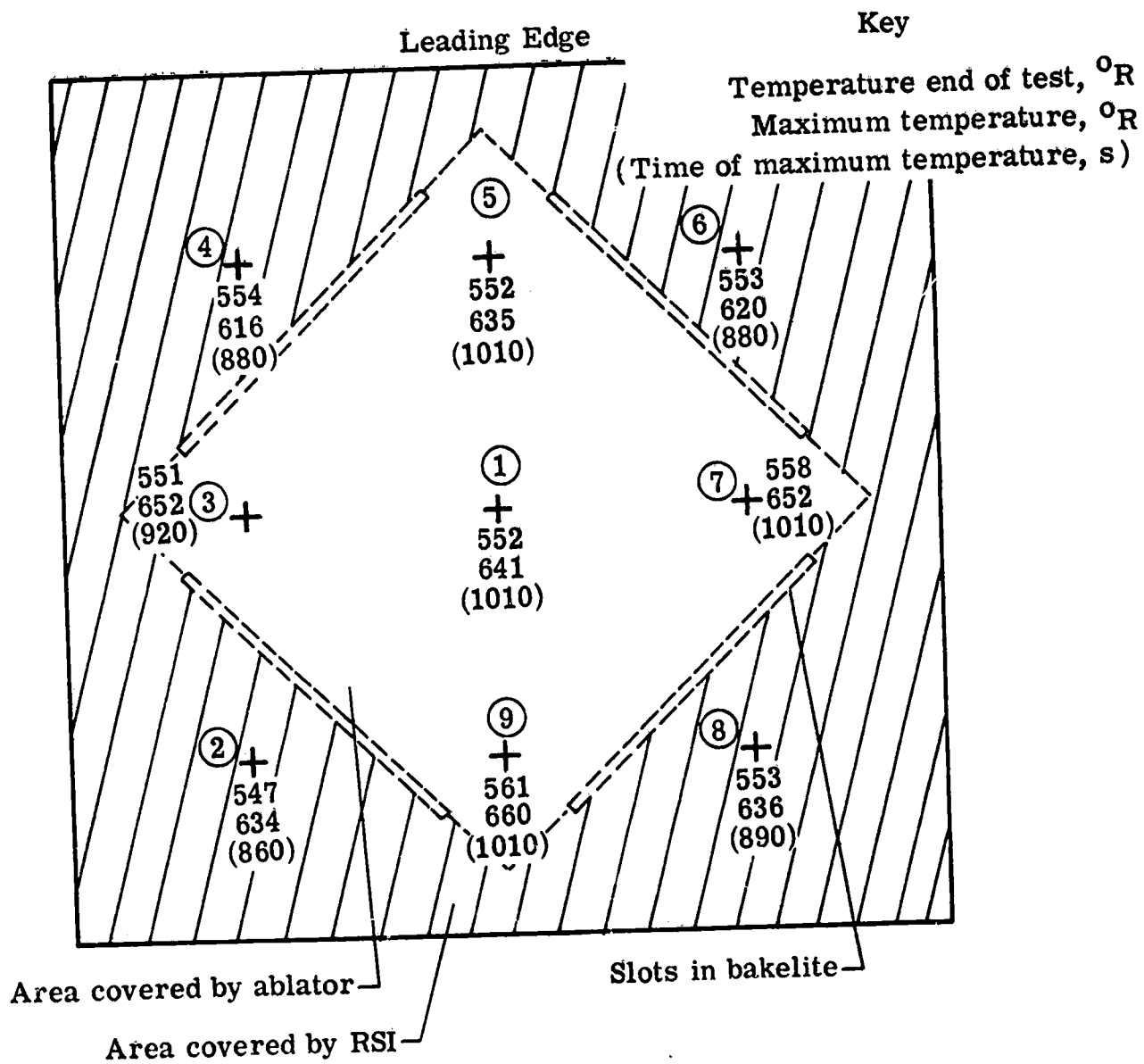
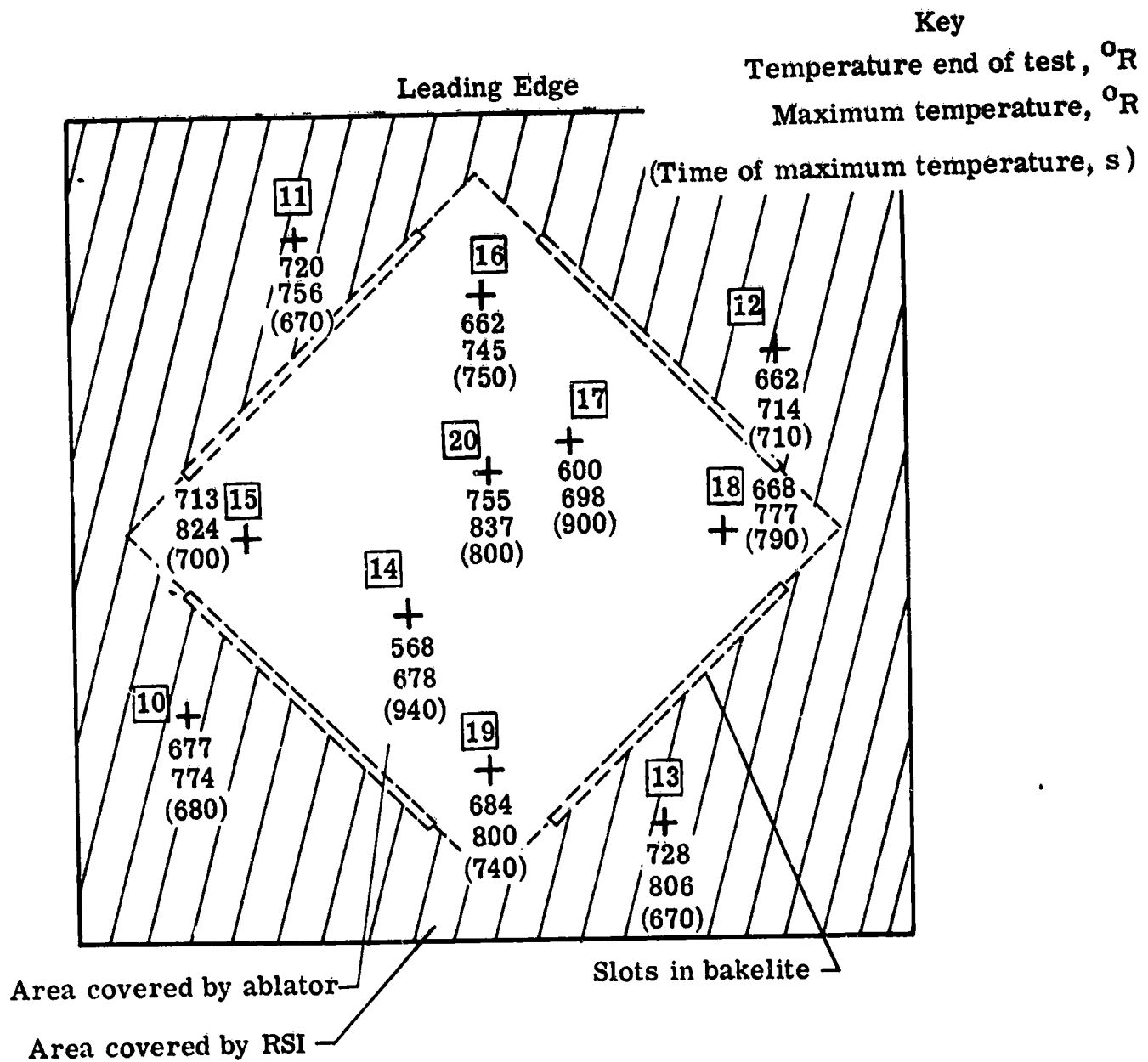


Figure 5.- Pressure port locations and typical pressure distributions (normalized to center point).



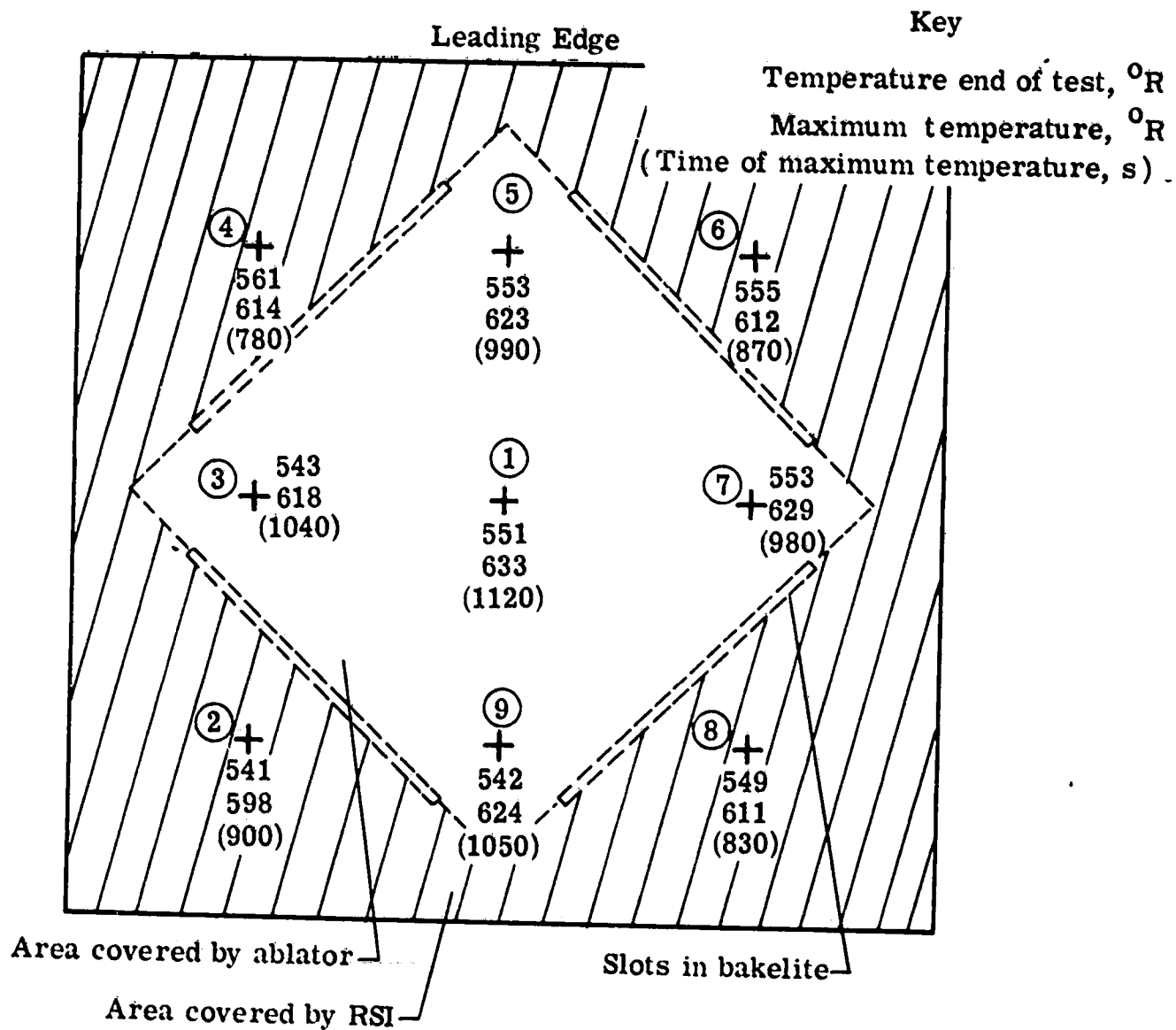
(a) Thermocouples located in carrier panel.

Figure 6 - Measured backsurface temperatures for ablator tile with plugged 3/16 inch hole tested at $q = 14 \text{ Btu/ft}^2\text{-s}$, $h_e = 1875 \text{ Btu/lbm}$ and $P_t = 0.038 \text{ atm}$ for 494s.



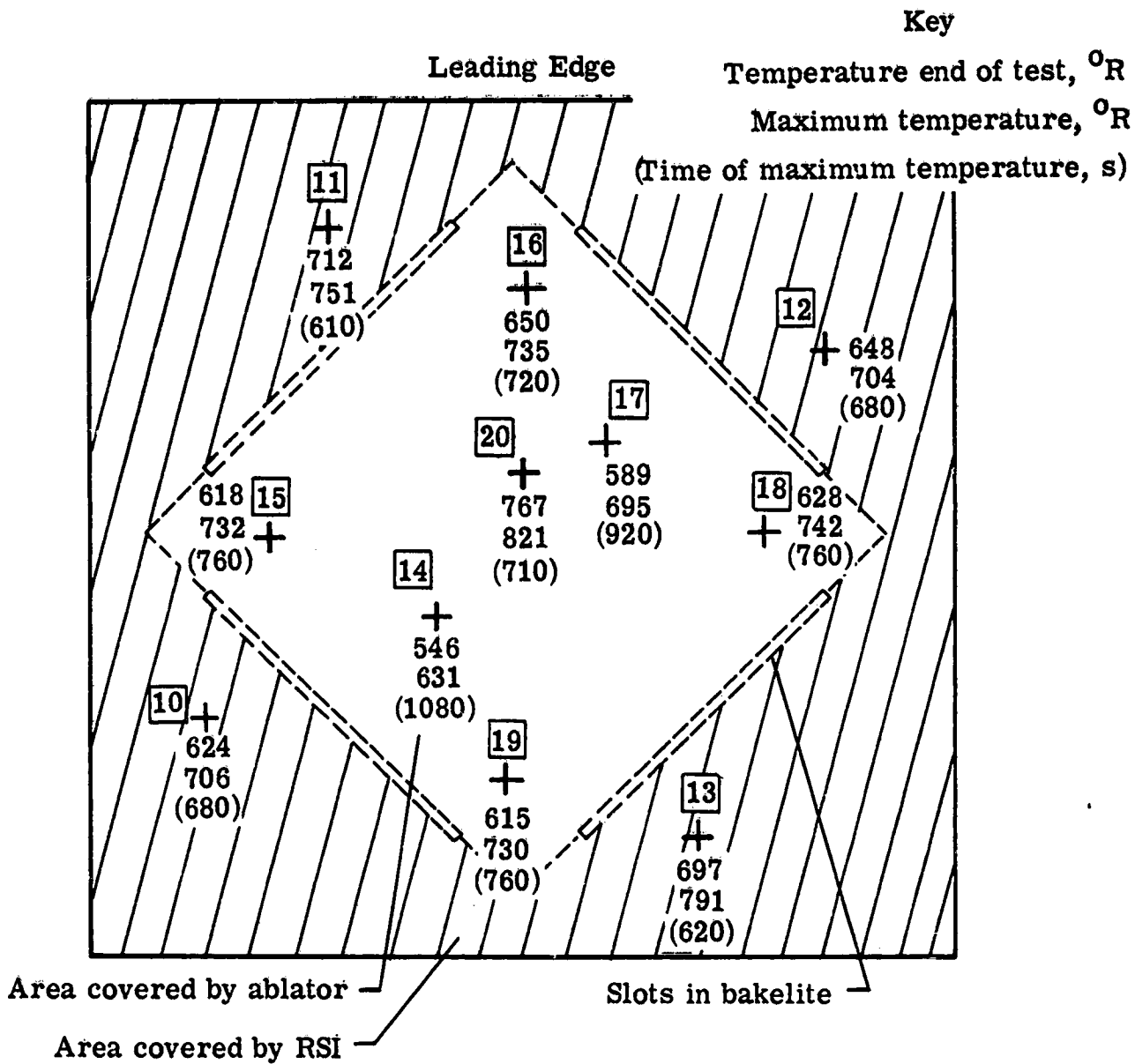
(b) Thermocouples located between SIP and ablator or RSI.

Figure 6 - Concluded.



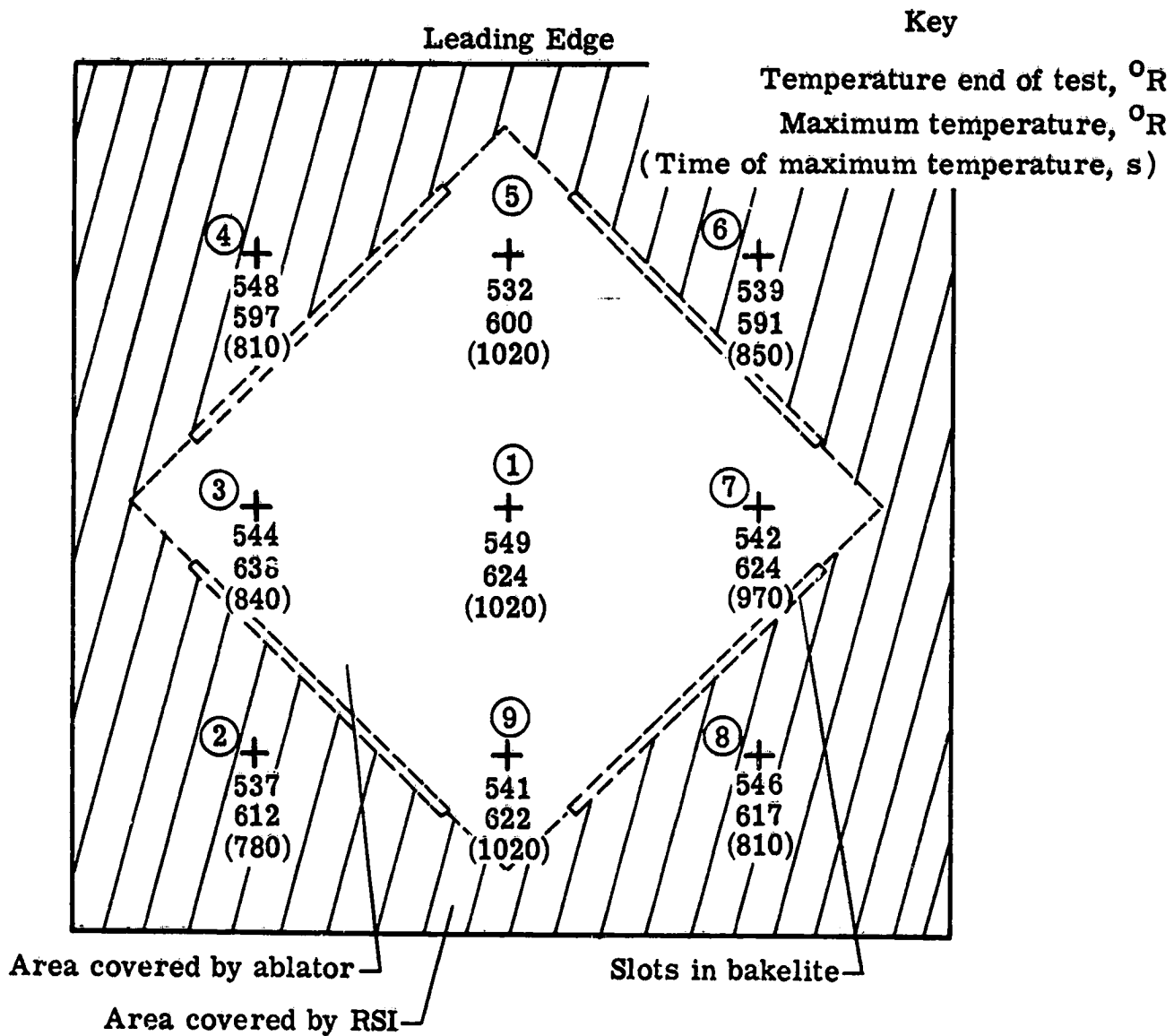
(a) Thermocouples located in carrier panel.

Figure 7 - Measured backsurface temperatures for ablator tile with 3/16 inch hole tested at $q = 14 \text{ Btu/ft}^2\text{-s}$, $h_e = 1875 \text{ Btu/lbm}$ and $P_t = 0.038 \text{ atm}$ for 450s.



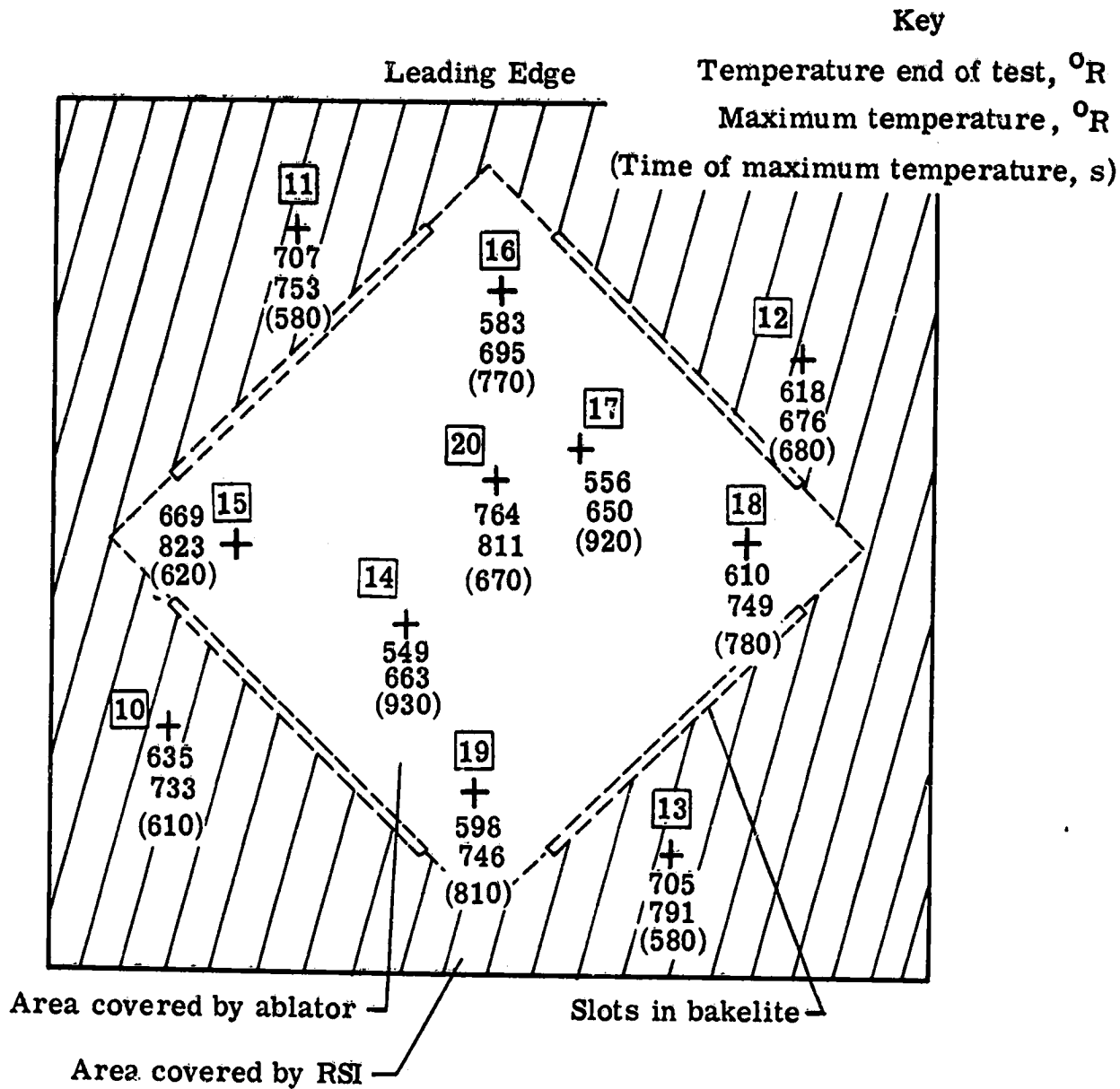
(b) Thermocouples located between SIP and ablator or RSI.

Figure 7 - Concluded.



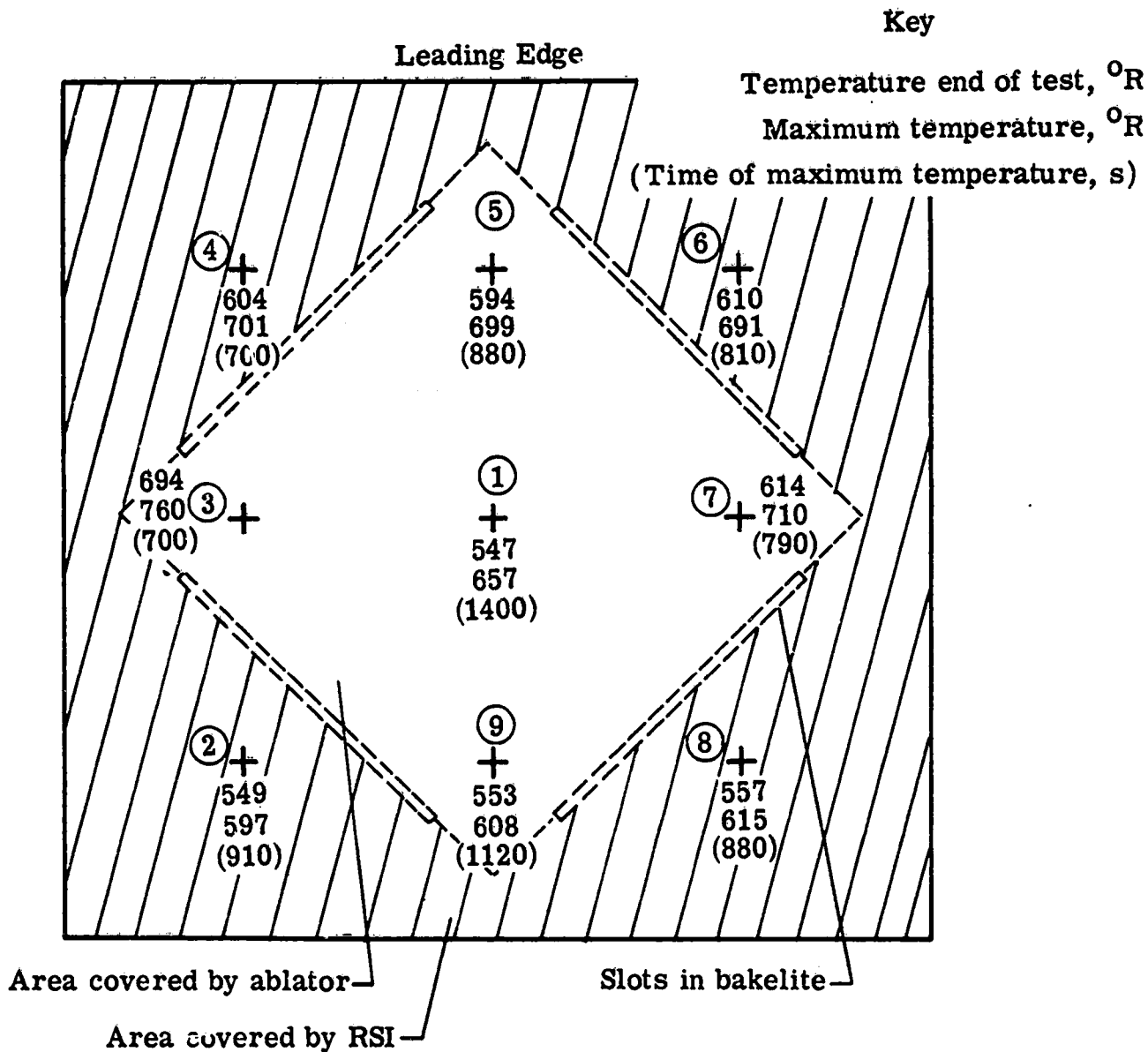
(a) Thermocouples located in carrier panel.

Figure 8 - Measured backsurface temperatures for ablator tile with 1/4 inch hole tested at $q = 14 \text{ Btu/ft}^2\text{-s}$, $h_e = 1875 \text{ Btu/lbm}$ and $P = 0.038 \text{ atm}$ for 420s.



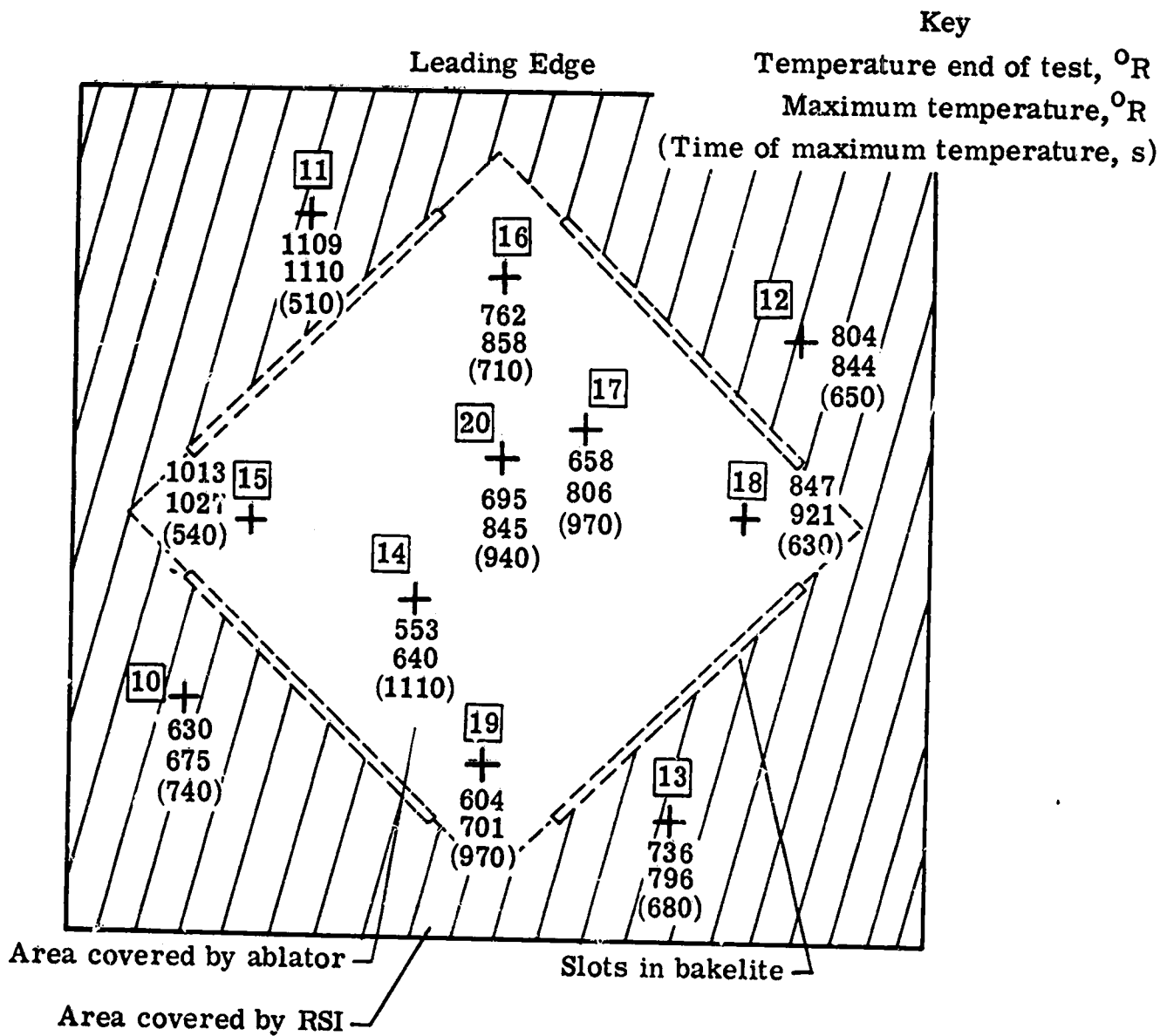
(b) Thermocouples located between SIP and ablator or RSI.

Figure 8 - Concluded.



(a) Thermocouples located in carrier panel.

Figure 9 - Measured backsurface temperatures for ablator tile with 3/16 inch hole plugged and ablator protruding 1/8 inch tested at $q = 14 \text{ Btu/ft}^2\text{-s}$, $h_e = 1875 \text{ Btu/lbm}$ and $P_t = 0.038 \text{ atm}$ for 500s.



(b) Thermocouples located between SIP and ablator or RSI.

Figure 9 - Concluded.

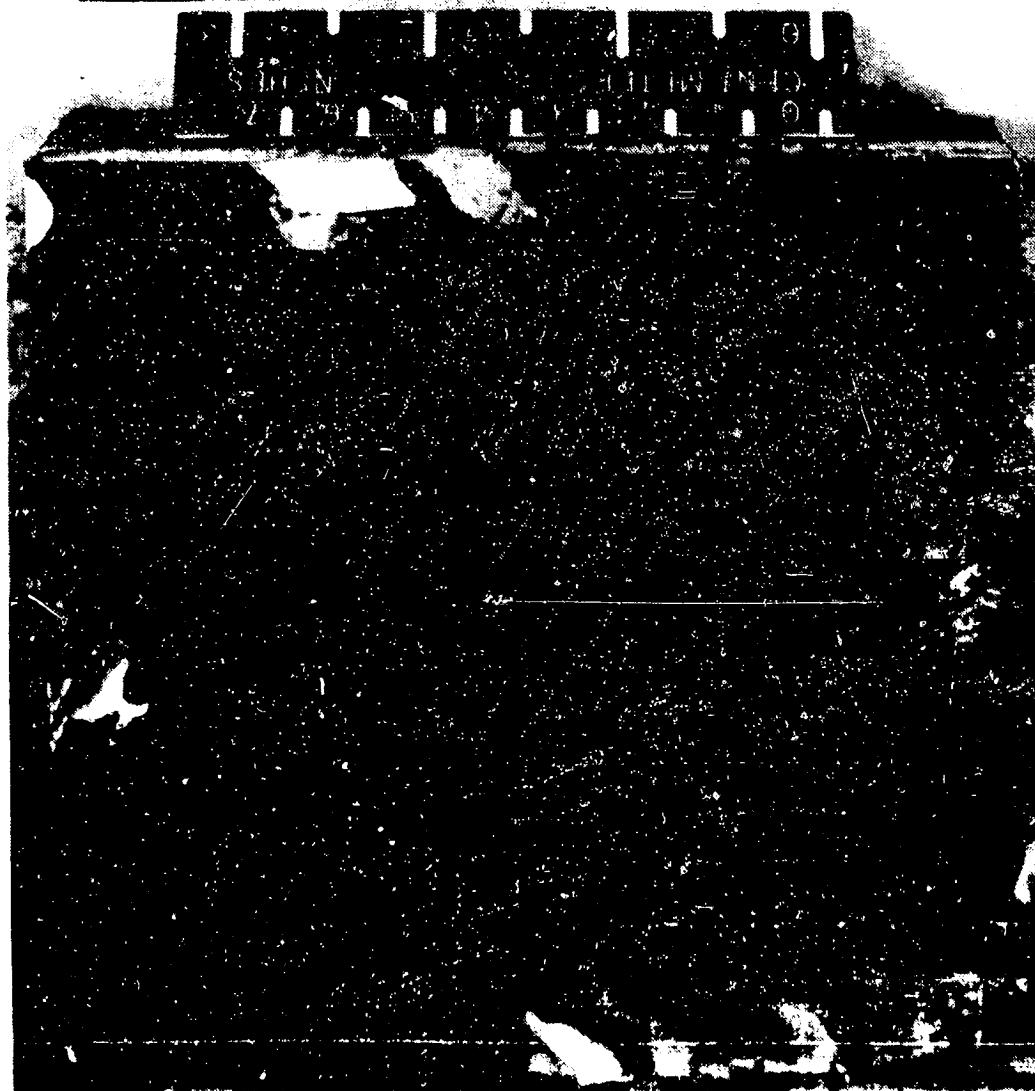
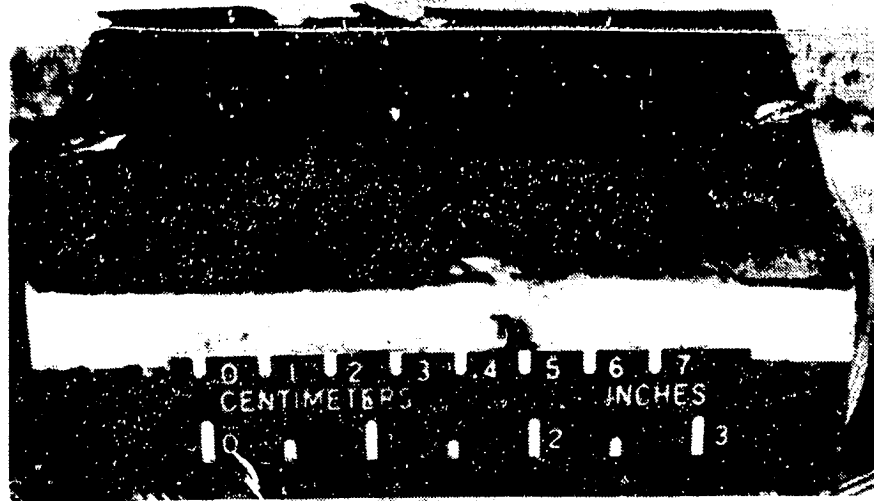


Figure 10. - Specimen with $3/16$ " physical hole, post test.

ORIGINAL IMAGE
OF PHOTO

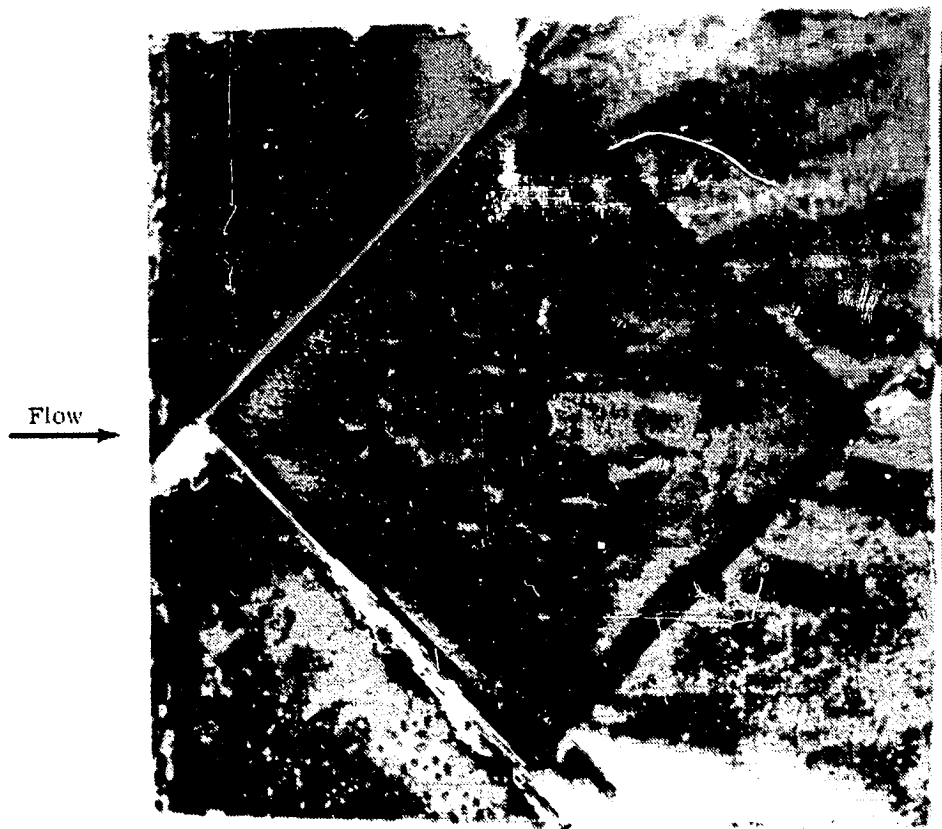


Figure 11. Specimen with 16" diameter hole, post test.

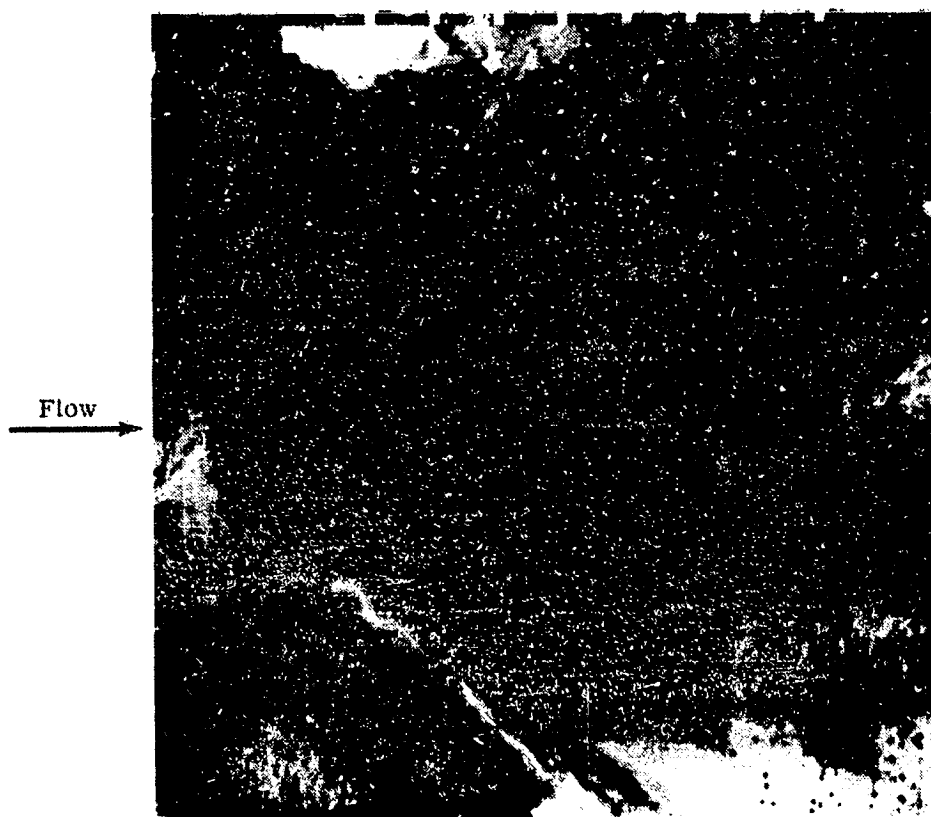
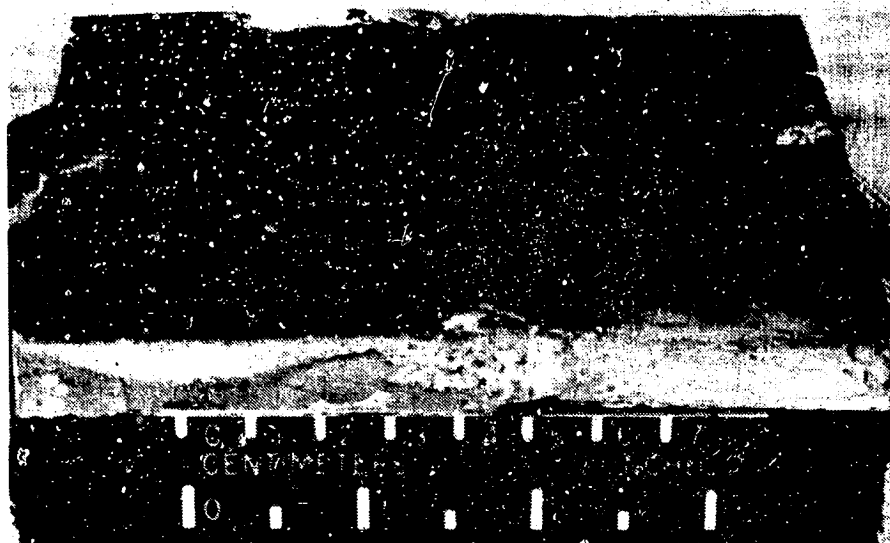


Figure 12.- Specimen with 1/4" diameter tool hole, post test.

**ORIGINAL PAGE IS
OF POOR QUALITY**

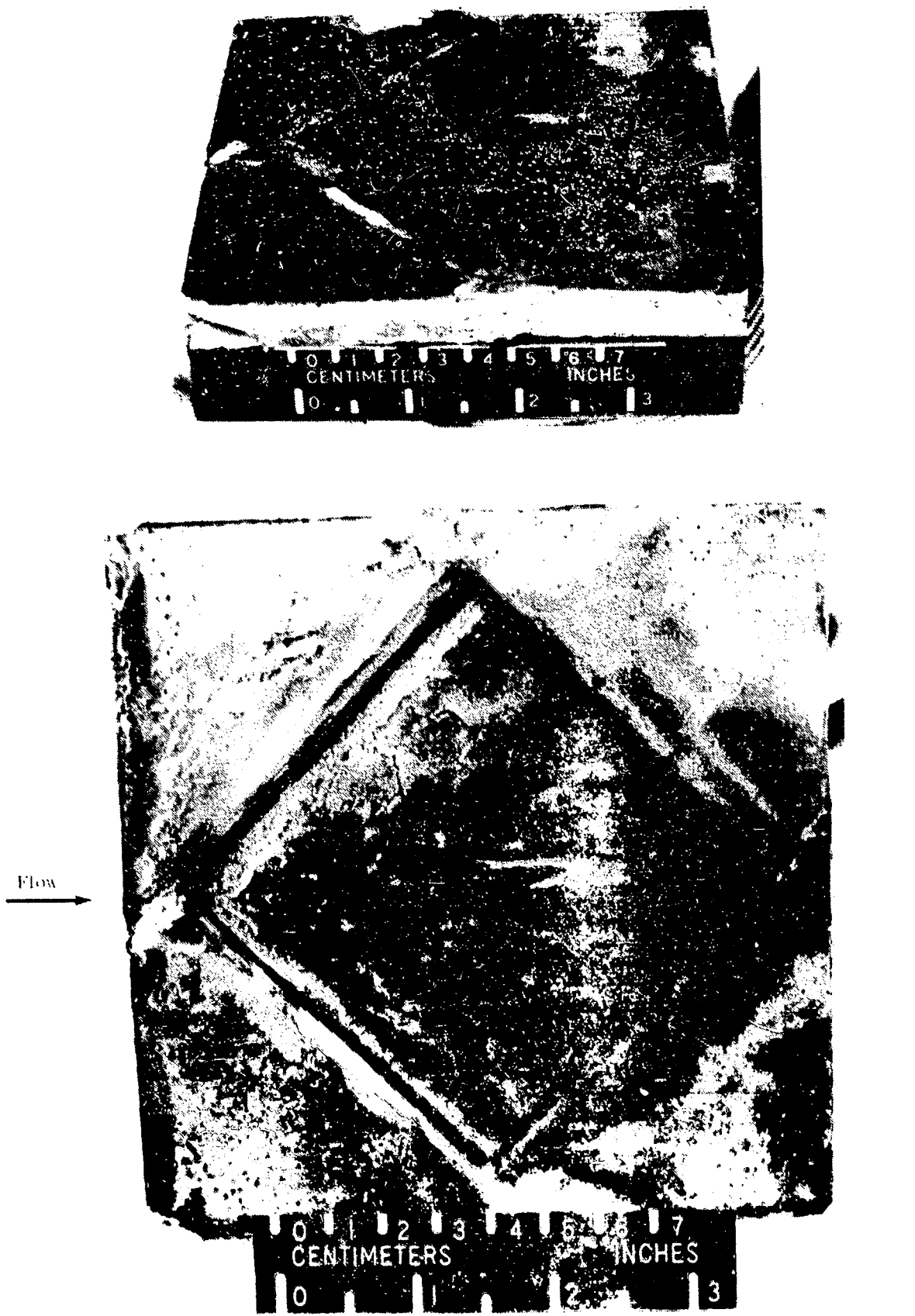
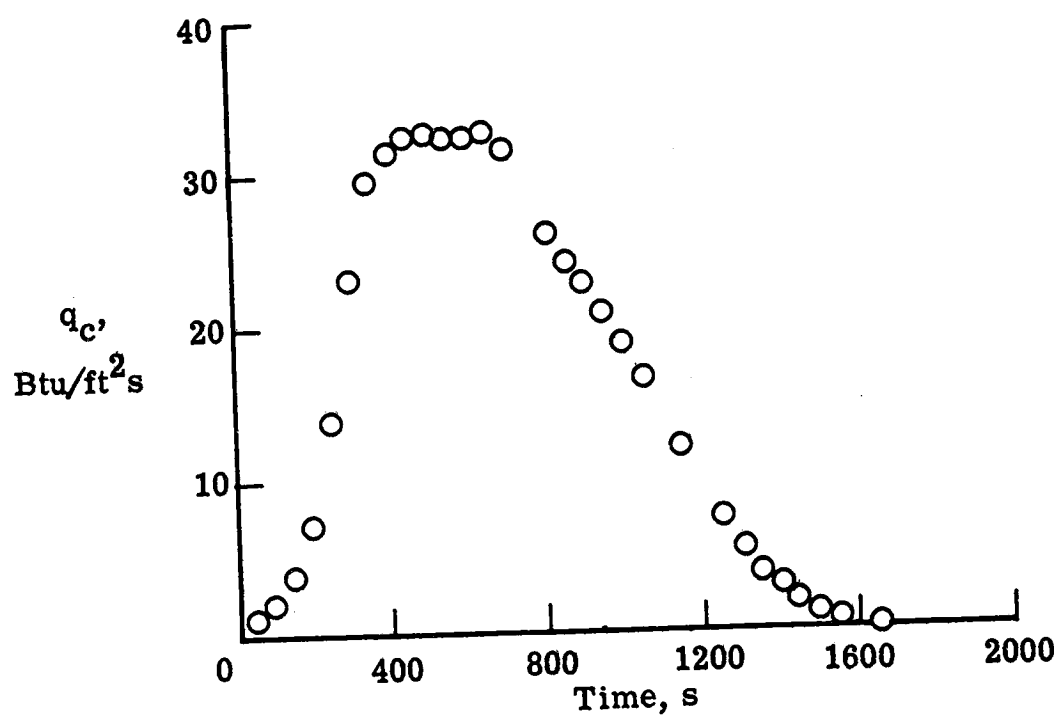
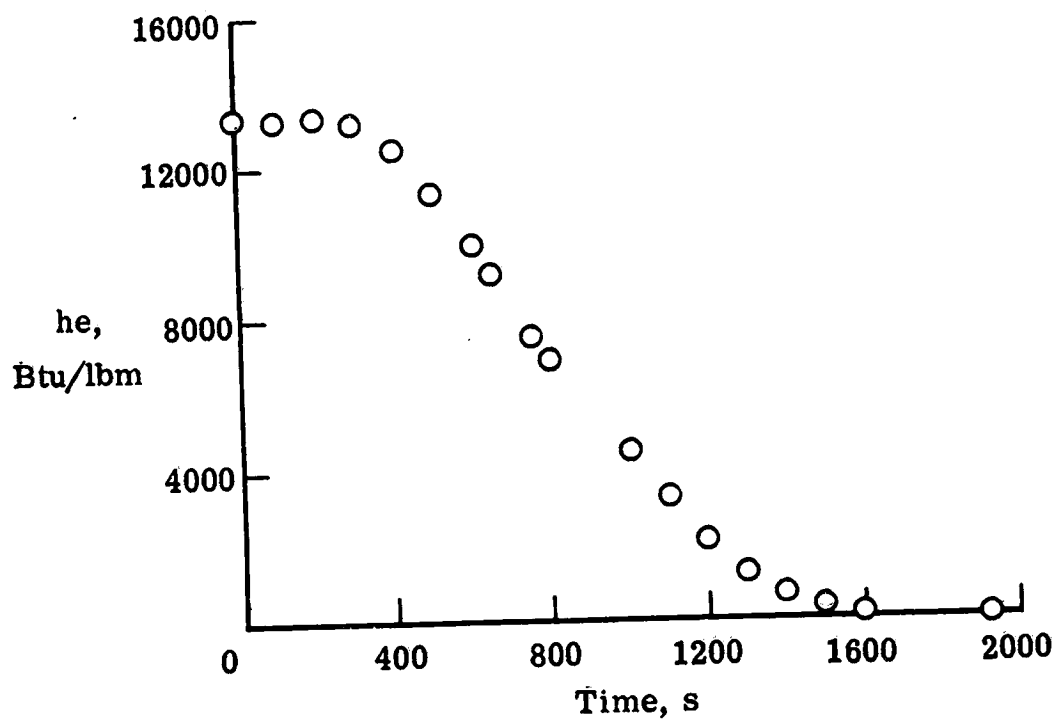


Figure 13. Specimen

post test.

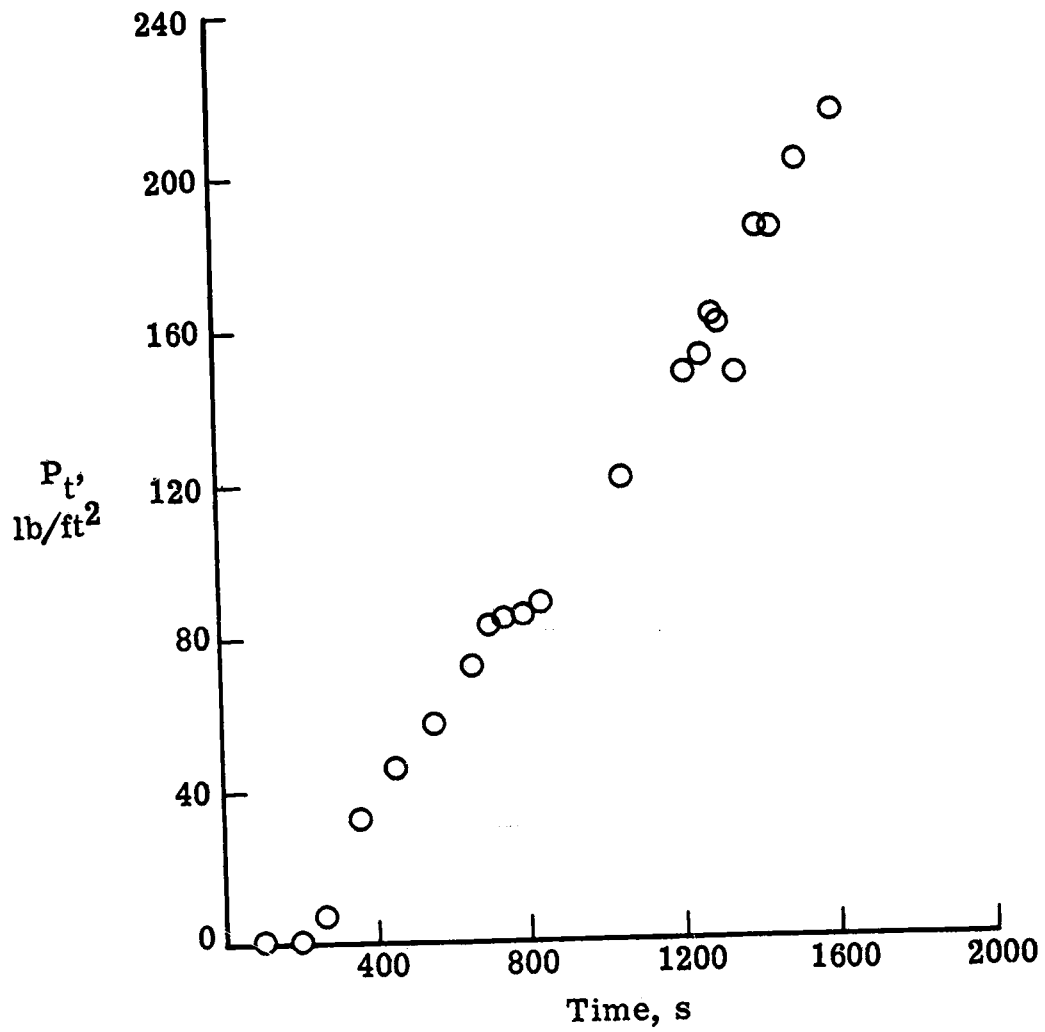


(a) Heating rate, body point 1030.

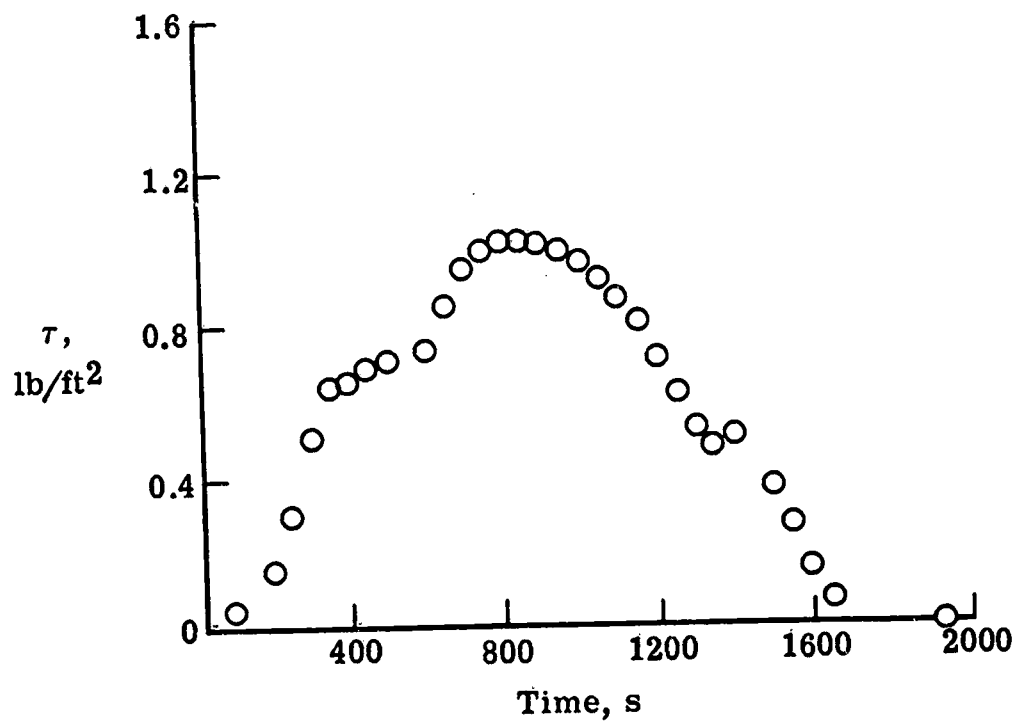


(b) Enthalpy, body point 1030.

Figure 14.- Predicted heating rate, enthalpy, pressure and shear for orbiter body point 1030, for the design entry trajectory 14414.1C.



(c) Pressure, body point 1030.



(d) Shear, body point 1030.

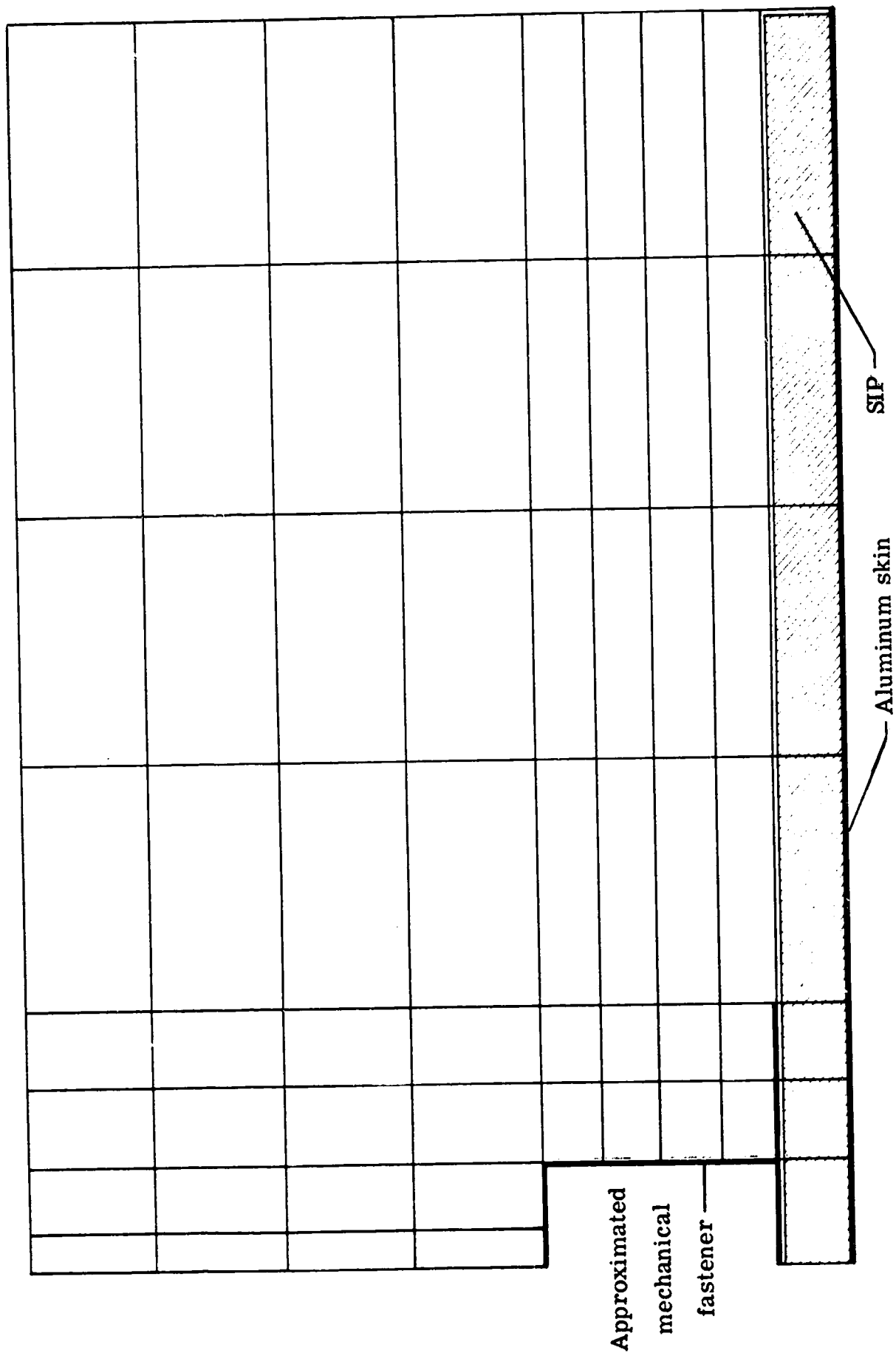


Figure 15 - Configuration used for two-dimensional analysis.

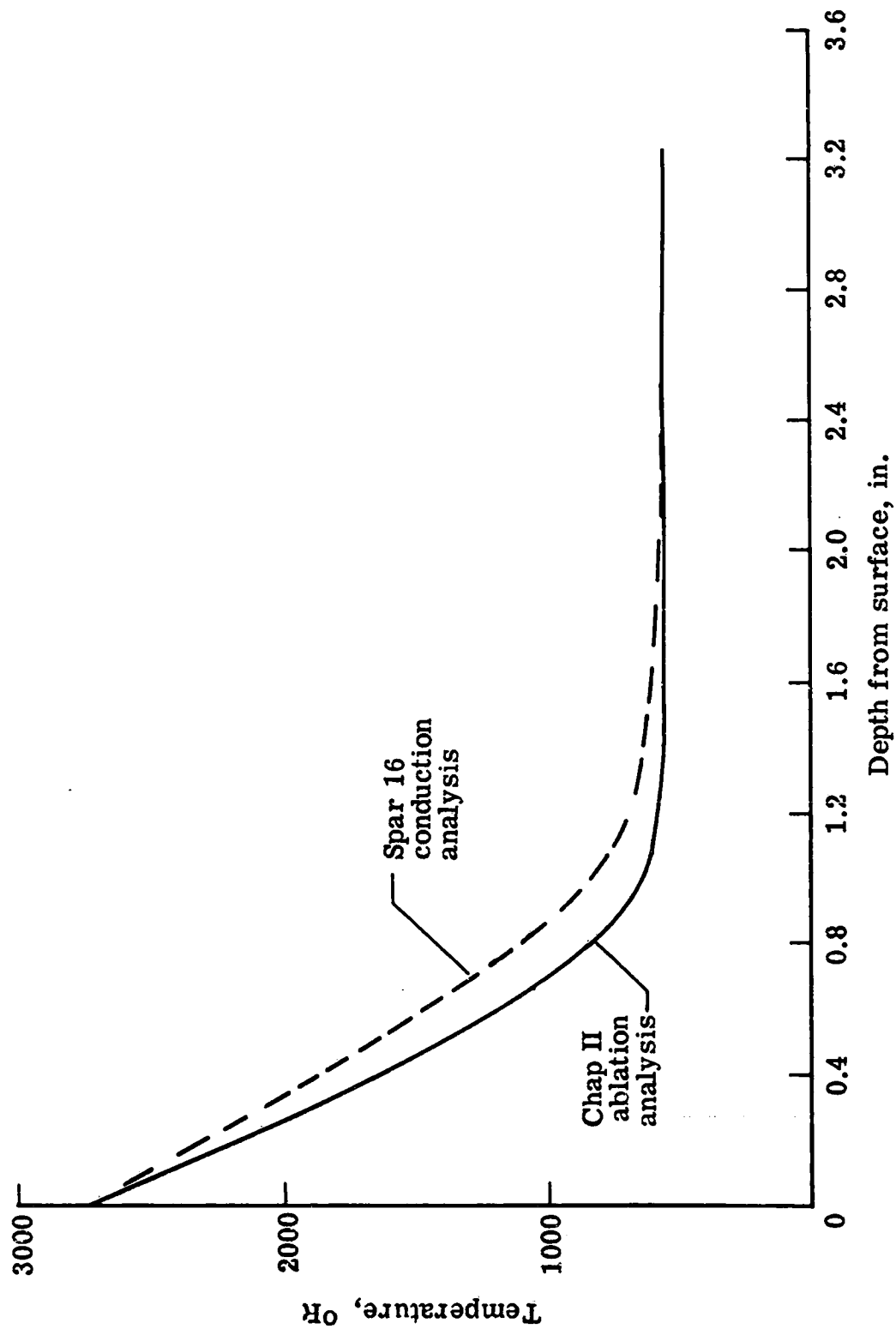
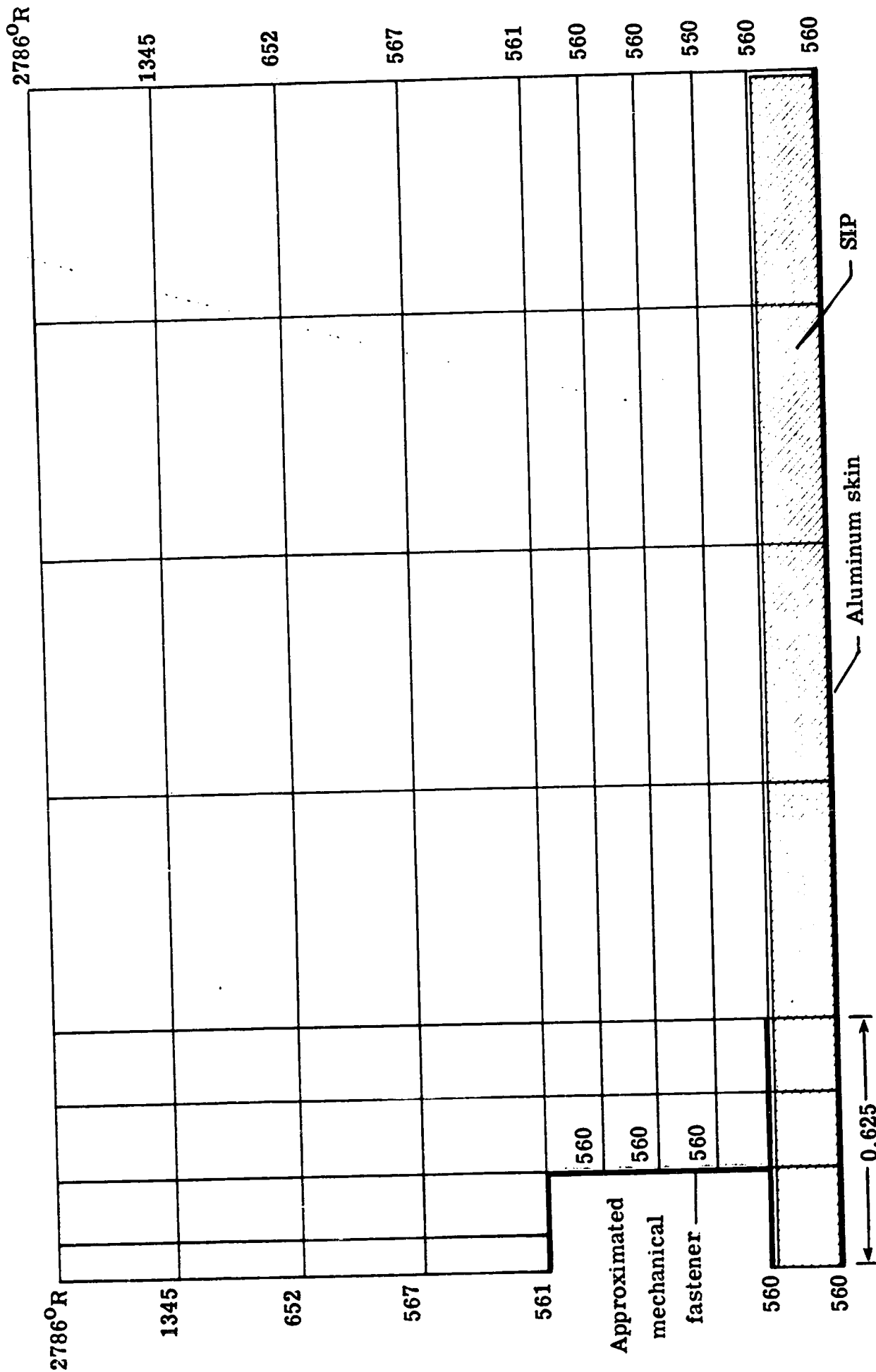


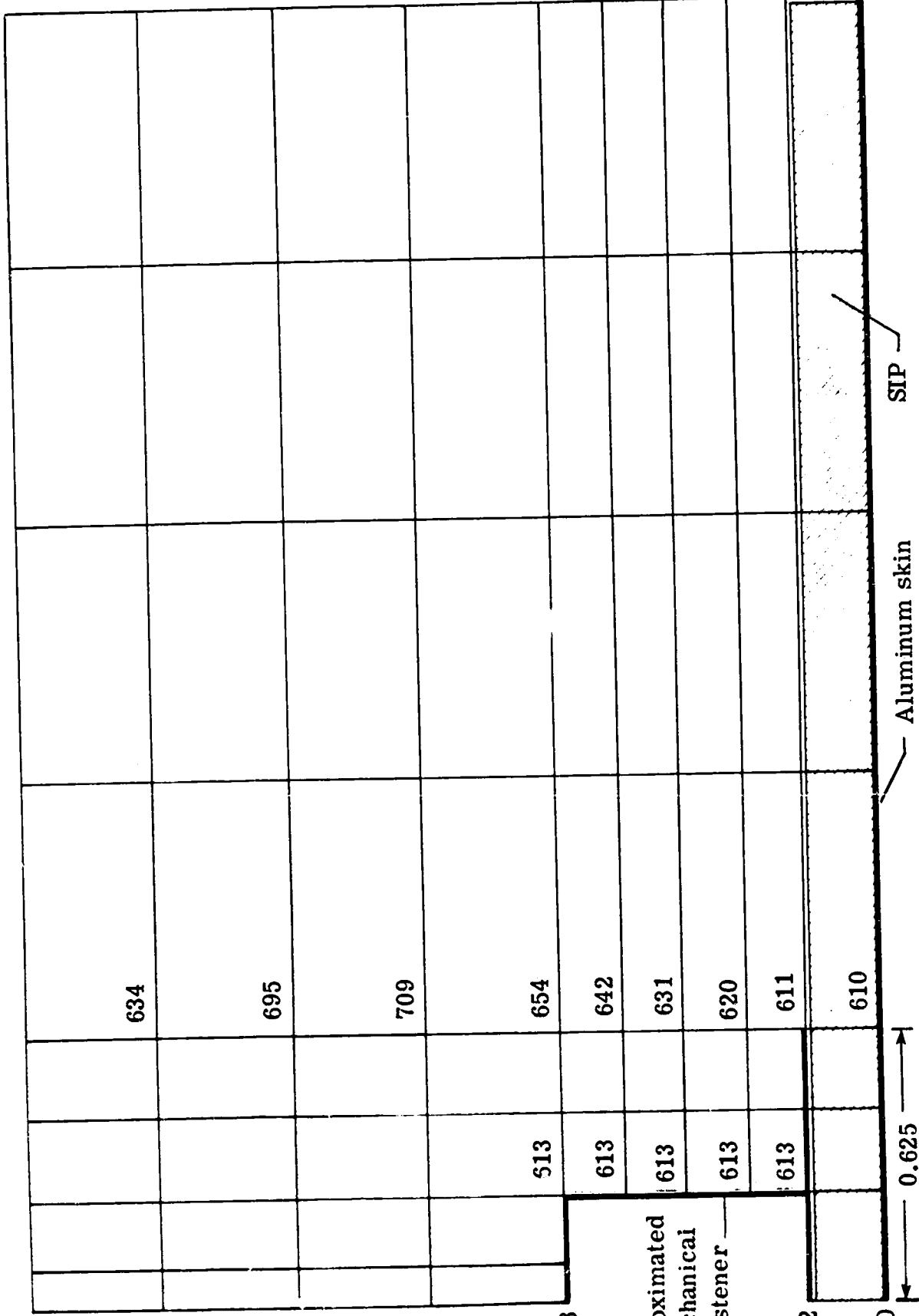
Figure 16.- Comparison of temperature distributions with one-dimensional and two-dimensional analyses for trajector 14414.1C body point 1030 (time of peak heating, 600s).



(a) At peak heating, 600s.

Figure 17 - Temperature distributions in SLA 561 tile with mechanical fastener for the design trajectory, 14414.1C.

547°R



547°R

634

695

708

613

Approximated mechanical fastener

612

610

634

695

709

513

613

613

613

613

0.625

Aluminum skin

SIP

610

(c) At 4000s.

Figure 17 - Concluded.